

- (4) Skolnick, J. *Macromolecules* 1984, 17, 645.
 (5) Zimm, B.; Bragg, J. *J. Chem. Phys.* 1959, 31, 526.
 (6) Abramowitz, M.; Stegun, I. A. "Handbook of Mathematical Functions with Formulas, Graphs, and Mathematical Tables"; Dover: New York, 1965; p 17.
 (7) Flory, P. "Statistical Mechanics of Chain Molecules"; Wiley: New York, 1969.
 (8) Poland, D.; Scheraga, H. A. "Theory of Helix-Coil Transitions in Biopolymers"; Academic Press: New York, 1970; Chapter 5.

Theory of the Kinetics of the Helix-Coil Transition in Two-Chain, Coiled Coils. 1. Infinite-Chain Limit

Jeffrey Skolnick[†]

Department of Chemistry, Washington University, St. Louis, Missouri 63130.
 Received November 16, 1983

ABSTRACT: The kinetics of the α -helix-to-random coil transition in two-chain, coiled coils (dimers) is examined in the context of a kinetic Ising model. We consider the dynamics of the helix-coil transition (or vice versa) of parallel, in-register dimers in which the effects of loop entropy are ignored. Focusing explicitly on homopolymeric chains, we have formulated a master equation for the mean occupation number of the j th residue q_j (equal to +1 (-1) for a completely helical (randomly coiled) state). Analytic expressions for the time dependence and equilibrium values of q_j are derived for the limiting cases of an isolated single chain as well as a DNA-isomorphic model (in which the instantaneous occupation numbers of the j th residue in both chains are identical) for chains of arbitrary length where the final state corresponds to $s = 1$ and $s(w^0)^{1/2} = 1$, respectively. Here, s is the Zimm-Bragg helix propagation parameter of a single residue and w^0 is the helix-helix interaction parameter. For infinite single chains and dimers having arbitrary initial and final states, we introduce physically reasonable approximations to close the infinite hierarchy of coupled differential equations involving multiple-site correlation functions of the occupation numbers. We then solve the resulting coupled first-order linear equations including all orders of two-site correlation functions for the time dependence of the mean occupation number. In the case of single chains an analytic expression for the slowest rate is derived and an examination of the time dependence of the normalized helix content, $H(t)$, is undertaken. In the case of two-chain, coiled coils, numerical results are presented for the time dependence of $H(t)$. A comparison is made of the time scale of the helix-coil transition in single chains and in dimers. Moreover, the validity of approximating $H(t)$ by the slowest relaxing mode is examined for the case of small and large perturbations from an initial state. We conclude that in the context of this model, in dimers this approximation is excellent over a wide variety of initial states and helix contents.

I. Introduction

Over the past several years an equilibrium statistical mechanical theory of the helix-to-random coil transition of α -helical, two-chain, coiled coils (dimers) has been developed.¹⁻⁴ The theory seems capable of rationalizing the enhanced stability of the two-chain, coiled coil relative to the isolated single chain (monomers) through the use of a helix-helix interaction parameter $w^{0,5,6}$ $-RT \ln w^0$ is the free energy of a positionally fixed, interacting pair of helical turns in the dimer relative to the free energy of the non-interacting, positionally fixed pair of helical turns in two isolated single chains. The equilibrium theory has been extended to include the effects of loop entropy^{2,3} and mismatch on the helix-coil transition⁴ and has been applied to the prototypical two-chain, coiled coil, the muscle protein tropomyosin, at near-neutral and at acidic pH.^{5,6} Thus, it seems reasonable at this time to begin an investigation of the kinetics of the helix-coil transition in two-chain, coiled coils; the present paper addresses itself to the preliminary treatment of the kinetics of such transitions.

While there is a sizeable body of experimental work characterizing the thermodynamic stability of tropomyosin and a synthetic analogue as a function of temperature,⁵⁻¹¹ the experimental situation with regard to the kinetics of the denaturation is not so sanguine. Although temperature-jump studies of tropomyosin have not been made, Tsong, Himmelfarb, and Harrington have studied the

melting kinetics of what they regard as structural domains in the myosin rod.¹² While our equilibrium picture is substantially different from theirs, nevertheless they extract relaxation times that experience a maxima as a function of temperature. The maximum occurs at the apparent midpoint of the transition, a situation reminiscent of that seen in the kinetics of the helix-coil transition in single-chain polypeptides.¹³ This is a very important feature which we believe any even qualitatively successful theory of the helix-coil transition must be able to duplicate.

There is a substantial collection of literature on the kinetics of the helix-coil transition employing the kinetic version of the Zimm-Bragg¹⁴ theory in single-chain polypeptides. Basically the approaches involve the solution of a master equation for a reduced probability distribution function or for a moment of the distribution function. In the former approach, one finds a coupled hierarchy of equations in which the $(n + 1)$ th-order distribution function is needed to find the n th-order distribution function. Typically, closure relations which are exact at equilibrium are introduced to truncate the hierarchy. These equations have been solved by employing doublet,¹⁵ triplet,¹⁶⁻¹⁸ quadruplet,¹⁹ and generalized closure schemes.²⁰⁻²⁴ Schwarz,^{13,23} Poland and Scheraga,²⁴ and Craig and Crothers²⁵ in particular have emphasized the importance of the initial slope as a well-defined rate constant for systems perturbed near as well as far from equilibrium. The initial rate treatment has been widely employed to interpret apparent approach to equilibrium measurements such as temperature jump,²⁵ ultrasonic

[†] Alfred P. Sloan Foundation Fellow.

absorption,^{27,28} and dielectric relaxation.^{29,30}

Pursuing a slightly different route, Tanaka, Wada, and Suzuki³¹ have solved for the autocorrelation function of the occupation numbers of the residue in an Ising model using an approximation to the third-order correlation function that is exact at zero time and at infinite time (equilibrium) to yield a closed, linearized set of equations. Later, Ishiwari and Nakajima³² employed the Tanaka-Wada-Suzuki method to simulate NMR relaxation spectra and examine the effect of polydispersity on α -CH NMR relaxation spectra.

Various approximate models have also been formulated. There is the zipper model developed by Chay and Stevens,³³ Miller,³⁴ and Jernigan, Ferretti, and Weiss.³⁵ This approach assumes that there is just a single helical sequence per chain, an approximation whose range of validity has been examined by Chay and Stevens.¹⁹ McQuarrie, McTague, and Reiss have treated the kinetics of the helix-coil transition assuming irreversible kinetics of denaturation or renaturation,³⁶ a questionable assumption under many circumstances. Clearly, then, the kinetics of the helix-coil transition in single chains has been the focus of considerable theoretical as well as experimental attention over the years.

Our objective here is to develop the simplest kinetic Ising model description of the helix-coil transition that retains the essence of what we believe are many of the important features of the physics and yet remains mathematically tractable. Thus, our first attempt incorporates the following features of the equilibrium situation.

(1) Within an individual chain, the theory is developed in terms of the Zimm-Bragg helix initiation parameter σ and propagation parameter s that are assumed to be characteristic of the individual amino acid in the chain and independent of the kind of nearest neighbors.¹⁴

(2) Interhelical interactions are accounted for by a parameter $w^{0,1-4}$

(3) The effects of loop entropy are ignored; that is, we a priori assign the statistical weight of unity to a randomly coiled residue independent of whether the randomly coiled residue occurs between interacting stretches of helices or not. At equilibrium, however, we have demonstrated that this approximation is in general incorrect;²⁻⁴ we retain it here because of the simplicity of the resulting equations. The theory in which loop entropy is ignored, the neglect-loop-entropy model, possesses many (but not all) of the qualitative features of the theory which incorporates loop entropy, the loops-excluded model. In the limit of sufficiently small σ , and in chains of short to moderate length, both theories give a single interacting helical stretch per molecule and are equivalent. As σ increases, the helix-coil transition predicted by the loops-excluded model will be more cooperative than that in the neglect-loop-entropy model. We shall clearly have to remove this approximation at a later date and ultimately incorporate into the theory the fact that loop entropy acts to produce a single interacting helical stretch per molecule.

(4) The two-chains are assumed to remain parallel and in-register throughout the course of the helix-coil transition; i.e., the possibility of mismatched association of the two-chains is entirely neglected. If interhelical interactions are responsible for the greatly augmented helix content of the dimer relative to the monomer, then in the limit of 100% helix, the in-register conformation completely dominates the population. However, as the chains melt, this is no longer likely to be so. The kinetic problem of jumping between various mismatched populations is a very complicated one. At this time we have no estimate whatsoever

of the mechanism or time scale of such jumps and thus are forced to make the simplest, bald approximation that there are just in-register states, thereby sidestepping the more general problem. Actually, however, if one is just looking at the kinetics of denaturation this approximation may not be too severe. However, the actual renaturation process will most certainly involve population rearrangements of out-of-register states.

(5) In the equilibrium theory we employed coarse graining as a physical statement that in order to effect the helix-helix interaction, residues a-d (e-g) of the quasi-repeating heptet must be in the all-helical state.³⁷⁻³⁹ Thus we partitioned the individual tropomyosin chains into alternating four- and three-residue blocks. Actually for the values of σ typical of proteins, the mean length of a helical state even in an isolated single chain is greater than four residues; thus calculations of the helix content of the dimer with and without coarse graining give identical results. For simplicity and to make contact with previous single-chain polypeptide work, coarse graining is neglected. Actually it is fairly straightforward to extend the model developed below to include coarse graining. It is apparent that on the basis of assumptions 1-5 we shall be formulating the kinetic Ising model version⁴⁰ of the perfect-matching-neglect-loop-entropy theory, the equilibrium theory of which has been developed previously.

We now present additional assumptions about the kinetics that are necessary for the development of the kinetic Ising model.

(1) The equilibrium parameters σ , s , and w^0 necessary to characterize the transition probabilities are characteristic of the equilibrium final state, an assumption taken to be true whether the final equilibrium state is near to or far from the initial state. On the likely time scale of the helix-coil transition of 10^{-4} - 10^{-5} s,¹² this is not an unreasonable assumption.

(2) We shall a priori assume that the transition probability, that is, the probability per unit time that the i th residue jumps from a state μ (+1 for helix, -1 for random coil) to state $-\mu$ depends on the state of the i th residue and its two nearest neighbors but does not depend symmetrically on the second-nearest-neighbor correlation between residues $i-1$ and $i+1$. This is equivalent to asserting that Schwarz's kinetic parameters γ_H and γ_C are both equal to $2/(1+\sigma)$.^{13,32} It should be pointed out that γ_H and γ_C have no equilibrium analogues and have no effect whatsoever on the final equilibrium state. However, different values of γ_H and γ_C do influence the rate of approach to equilibrium. The values of γ_H and γ_C we have chosen give rise to the simplest description of the kinetics.

(3) We shall assume that the kinetics of the helix-coil transition in dimers is not diffusion controlled. This is most reasonable for the kinetics of denaturation of the two-chain, coiled coil in which (at higher values of the helix content at least) the chains start out completely associated. As the temperature is raised and as the helix content decreases, the fraction of single chains increases. We shall assume that as the dimer melts, one can follow the time course of the melting of that particular dimer without regard to the association-dissociation equilibrium. Similarly, for renaturation, we are assuming that the diffusion of the two chains to each other is so fast on the scale of the kinetics of the helix-coil transition that the internal helix-coil dynamics is the rate-determining step. Of course, as the concentration of chains goes to zero, this cannot be correct. In essence then, we can imagine that we are studying the kinetics of two-chains linked by a benign tether or molecular staple that has no effect on the

dynamics or equilibrium properties other than to keep the centers of mass of the two-chains near each other.

In the context of this simplest model of the kinetics of the helix-coil transition, we wish to pose several qualitative questions and in the body of the paper provide qualitative answers. First, what is the time scale of the kinetics of the helix-coil (or coil-helix) transition in the dimer as compared to the time scale in the isolated single chains? Does the mean relaxation time characterizing the approach to the final, infinite time, equilibrium state have a maximum at the midpoint of the helix-coil transition? If so, what is (are) the underlying physical origin(s) of such a maximum? How does the time scale for the approach to the $t = \infty$ state differ between a small perturbation from the initial state and a large perturbation from the initial state? It is to the aforementioned questions that the remainder of this paper addresses itself.

In section II, the Ising model of the two-chain, coiled coil is formulated. We begin with the construction of the free energy of a dimer in terms of the instantaneous occupation number of each of the residues. Using detailed balance we derive the transition probability for the j th residue. Then following the prescription of Glauber,⁴⁰ we derive a master equation for the time dependence of the mean occupation number $\langle \mu_j \rangle = q_j$. A discussion of the relationship of the kinetic neglect-loop-entropy model and the DNA-isomorphic model in which the instantaneous state of the j th residue in both chains is taken to be identical is presented. (We point out that the DNA-isomorphic model is of interest in that it is formally equivalent to the single-chain kinetic Ising model.) Various limiting cases are discussed.

In section III, approximate master equations for the average occupation number of the j th residue in an infinite, isolated single chain as well as in two-chain, coiled coils are derived and solved for the time dependence of the mean occupation number. In the case of single chains, an exact analytic expression for the eigenvectors and eigenvalue corresponding to the slowest relaxing mode valid over a wide range of helix content is calculated. In the more complicated case of dimers, while no analytic solution has been found, forms suitable for numerical analysis are presented.

In section IV, numerical results for the kinetics of the helix-coil transition are presented. In the case of single chains, various calculations as a function of different initial and final states for $\sigma = 10^{-4}$ are examined. In the case of dimers, we demonstrate that the kinetic model reduces to the single-chain limit when $w^0 = 1$, that is, when there are no interhelical interactions. We then examine the kinetics of the helix-coil transition as a function of w^0 for initial states near and widely separated from the final state and compare relaxation spectra probed in the single chains and two-chain, coiled coils. Finally section IV summarizes the conclusions of the present work and points out several possible directions for future research.

II. General Formulation of Perfect-Matching, Neglect-Loop-Entropy Kinetic Ising Model

General Considerations: Single Chains. Consider an isolated single chain composed of $N - 1$ residues; let the conformational state residue of the k th residue be characterized by an occupation number, μ_k ;

$$\mu_k = +1 \quad \text{if the } k\text{th residue is helical} \quad (\text{II-1a})$$

$$\mu_k = -1 \quad \text{if the } k\text{th residue is randomly coiled} \quad (\text{II-1b})$$

i.e., we have a one-dimensional kinetic Ising model. Fol-

lowing Glauber,⁴⁰ Tanaka, Wada, and Suzuki,³¹ and Ishiwari and Nakajima,³² the free energy (in the case of a magnetic system, the Hamiltonian) is given by

$$\mathcal{H}_1 = -\sum_{k=1}^N J_k \mu_k \mu_{k-1} - \sum_{k=0}^N H_k \mu_k \quad (\text{II-2})$$

where J_k reflects the cooperativity between units and H_k reflects the free energy difference between the +1 and -1 states. We shall assume the chain is homopolymeric and thus J_k and H_k are independent of position. Furthermore, for chains of finite length, we have to add two phantom coil units at the chain ends to complete the isomorphism between the Ising model and standard helix-coil transition theory. That is

$$\mu_0 = \mu_N = -1 \quad (\text{II-3})$$

By examining the statistical weight of the three consecutive randomly coiled residues (-1, -1, -1) as compared to the statistical weight of three consecutive helical states, (1, 1, 1) it follows that

$$\sigma = e^{-4J/k_B T} \quad (\text{II-4a})$$

$$s = e^{2H/k_B T} \quad (\text{II-4b})$$

Here, k_B is Boltzmann's constant and T is the absolute temperature. As shown in Appendix A, the Ising model employed here is isomorphic with the Zimm-Bragg model and thus previous calculations can be employed to construct equilibrium averages.

General Considerations: Two-Chain, Coiled Coils.

Consider now the analogous expression to eq II-2 for a two-chain, coiled coil containing $N - 1$ residues per chain that experiences an enhanced helix stability only when the residues in each of the two-chains are helical. We can write for the free energy of the homopolymeric dimer

$$\mathcal{H}_{12} = \mathcal{H}_1 + \mathcal{H}_1^0 - Q \sum_{j=1}^{N-1} (1 + \mu_j)(1 + \mu_j^0) \quad (\text{II-5})$$

with \mathcal{H}_1 and \mathcal{H}_1^0 the free energy of noninteracting chains 1 and 2. Q is the interchain interaction parameter that expresses the preference for the helix-helix state in both chains. In eq II-5 and all that follow a superscript zero refers to chain two; e.g., μ_j^0 is the occupation number of the j th residue in chain two. Nonsuperscripted variables (e.g., μ_j) refer to chain one.

w^0 is related to Q by considering the statistical weight of three helical residues in both chains in a dimer, each chain of which contains three real residues plus the two appended phantom units as compared to the all random coil state. We find

$$w^0 = \exp[4Q/k_B T] \quad (\text{II-6})$$

As a shorthand notation let us denote the collection of occupation numbers $\{\mu_i\}$, $i = 0, N$, in chain one by μ and $\{\mu_i^0\}$, $i = 0, N$, in chain two by μ^0 .

Construction of the Master Equation. Now, let $P(\mu, \mu^0, t)$ be the instantaneous probability that the two-chain, coiled coil has state μ in chain one and μ^0 in chain two at time t . Moreover, let $\omega(\mu_j)$ be the probability per unit time that the j th occupation number flips from μ_j to $-\mu_j$, while all the other spins remain momentarily fixed. We further assume $P(\mu, \mu^0, t)$ obeys the following master equation:

$$\frac{dP(\mu, \mu^0, t)}{dt} = \sum_{j=1}^{N-1} -(\omega(\mu_j) + \omega(\mu_j^0))P(\mu, \mu^0, t) + \omega(-\mu_j)P(\mu_1, \dots, -\mu_j, \dots, \mu_{N-1}, \mu^0, t) + \omega(-\mu_j^0)P(\mu, \mu_1^0, \dots, -\mu_j^0, \dots, \mu_{N-1}^0, t) \quad (\text{II-7})$$

If eq II-7 could be solved exactly we would have the most detailed description of the dynamics consistent with this master equation. Unfortunately, except for a few limiting cases, no exact solution has been achieved.

Construction of the Transition Probability $\omega(\mu_j)$. Define $p_j(\mu_j)$ ($p_j(\mu_j^0)$) as the equilibrium probability that the j th residue in chain one (two) has the value μ_j (μ_j^0). Assuming detailed balance gives

$$\frac{\omega(\mu_j)}{\omega(-\mu_j)} = \frac{p_j(-\mu_j)}{p_j(\mu_j)} \quad (\text{II-8a})$$

Employing eq II-5 in eq II-8a results in

$$\frac{\omega(\mu_j)}{\omega(-\mu_j)} = \frac{\exp\left\{-\frac{J}{k_B T}\mu_j(\mu_{j+1} + \mu_{j-1}) - \frac{H}{k_B T}\mu_j - \frac{Q}{k_B T}\mu_j(1 + \mu_j^0)\right\}}{\exp\left\{\frac{J}{k_B T}\mu_j(\mu_{j+1} + \mu_{j-1}) + \frac{H}{k_B T}\mu_j + \frac{Q}{k_B T}\mu_j(1 + \mu_j^0)\right\}} \quad (\text{II-8b})$$

Following the method of Glauber,⁴⁰ we choose

$$\omega(\mu_j) = \frac{\alpha}{2} \left\{ 1 - \frac{\gamma}{2}\mu_j(\mu_{j+1} + \mu_{j-1}) \right\} \{1 - \delta\mu_j\mu_j^0\} \{1 - \beta\mu_j\} \quad (\text{II-9a})$$

with a similar expression for $\omega(\mu_j^0)$ obtained from eq II-9a by interchanging the superscripted and nonsuperscripted occupation numbers. In eq II-9a, α has dimensions of time⁻¹ and sets the fundamental time scale for the process. α corresponds to the fundamental conformational jump time between a single helix and coil state in the absence of cooperativity. Moreover

$$\gamma = \tanh(2J/k_B T) = (1 - \sigma)/(1 + \sigma) \quad (\text{II-9b})$$

$$\delta = \tanh(Q/k_B T) = ((w^0)^{1/2} - 1)/((w^0)^{1/2} + 1) \quad (\text{II-9c})$$

$$\beta = \tanh\left(\frac{H + Q}{k_B T}\right) = (s(w^0)^{1/2} - 1)/(s(w^0)^{1/2} + 1) \quad (\text{II-9d})$$

γ and δ play the role of intrachain and interchain cooperativity parameters, respectively. On setting $w^0 = 1$ in eq II-9c and II-9d, we recover the transition probability for the isolated single-chain polypeptide derived previously by Glauber for a one-dimensional spin system.⁴⁰

Expectation Values of the Occupation Numbers.

We shall define $q_j(t)$ (q_j^0) to be the expectation value of μ_j (μ_j^0) which is regarded as a stochastic function of time;

$$q_j(t) = \sum_{\mu, \mu^0} \mu_j(t) P(\mu, \mu^0, t) \quad (\text{II-10})$$

the index μ, μ^0 implies that the sum is to be carried out over all the 4^{N-1} possible values of the occupation numbers of the residues in the dimer. We shall also require the expectation values of the two-site occupation numbers

$$r_{jk} = \langle \mu_j(t) \mu_k(t) \rangle = \sum_{\mu, \mu^0} \mu_j \mu_k P(\mu, \mu^0, t) \quad (\text{II-11a})$$

$$r_{jk^0} = \langle \mu_j(t) \mu_k^0(t) \rangle = \sum_{\mu, \mu^0} \mu_j \mu_k^0 P(\mu, \mu^0, t) \quad (\text{II-11b})$$

Observe that

$$r_{jj}(t) = 1 \quad (\text{II-11c})$$

As has been pointed out by Glauber, by determining the various moments of $P(\mu, \mu^0, t)$, we are merely constructing a moment expansion of $P(\mu, \mu^0, t)$, a standard technique for solving a master equation.⁴⁰

Using the definition of $q_j(t)$ in eq II-10 and employing the transition probability of eq II-9a, it is straightforward to show that $q_j(t)$ obeys the master equation

$$dq_j/dt = -2\langle \mu_j(t) \omega(\mu_j(t)) \rangle \quad (\text{II-12a})$$

$$\alpha^{-1} \frac{dq_j}{dt} = - \left\{ (1 - \delta)q_j - \frac{\gamma}{2}(q_{j-1} + q_{j+1}) + \frac{\gamma\delta}{2} (\langle \mu_j \mu_j^0 \mu_{j-1} \rangle + \langle \mu_j \mu_j^0 \mu_{j+1} \rangle) - \beta + \frac{\beta\gamma}{2}(r_{j,j-1} + r_{j,j+1}) + \beta\delta r_{j,j^0} - \frac{\beta\gamma\delta}{2}(r_{j-1,j^0} + r_{j+1,j^0}) \right\} \quad (\text{II-12b})$$

Equation II-12b is to be solved subject to the boundary conditions that $q_0 = q_N = -1$ at all times.

It should be pointed out that the initial slope of $q_j(t)$ vs. t is trivially and exactly obtained from eq II-12b provided that the initial values of the one-site, two-site, and three-site correlation functions are specified. Assuming that before the perturbation is applied, the system can be characterized by an equilibrium distribution, all the various correlation functions can be calculated and thus the initial slope can be exactly determined.

Let us consider the physical meaning of eq II-12b. Since the helix-coil transition is cooperative, we would expect that the kinetics will depend not only on the state of residue j but also explicitly on residues $j \pm 1$, as well as the state of neighboring residues in the other chain. Thus, q_j depends implicitly on the state of all the residues in the chain. Suppose $\beta = \delta = 0$; i.e., we have a single chain whose equilibrium helix content in the limit of infinite chain length is 50%, that is, in $q_{j-1} = q_{j+1} = q_j = 0$. Equation II-12b states that the average rate of change in q_j depends only on the state of q_j , its two nearest neighbors $q_{j\pm 1}$, and the value of the cooperativity parameter σ (see eq II-9b). Hence the rate of approach to equilibrium is slower than if $\gamma = 0$ (i.e., $\sigma = 1$). Setting β and $\delta \neq 0$ means that the statistical weights of coil and helix states are no longer identical and there is an added bias toward a given state (helix or coil). Now q_j depends on the state of the nearest neighbors as seen in the terms $r_{j,j-1}$ and on the state of the residue in the neighboring chain, e.g., $\langle \mu_j^0 \mu_{j\pm 1} \rangle$. The rates of decay of these higher order correlation functions in turn depend on the decay of even higher order correlation functions; this results in an infinite hierarchy of first-order equations. Except for special cases no exact solution is known. Equation II-12b embodies the simplest description of how the j th helical state can change in time. Finally, since there are two ways for r_{jk} to change, e.g., $ch \rightarrow cc$ or hh , these higher order correlation functions decay faster. Hence the rate of approach to equilibrium will be slowest when $\beta = 0$ and therefore can only increase for nonzero values of β . Since δ couples the dynamics of the two-chains and it plays the role of an interchain cooperativity parameter, a nonzero value of δ acts to decrease the rate of change of q_j (see below).

In writing eq II-12b we have used the fact that the two-chains are identical and thus $q_j = q_j^0$. The solution of eq II-12b constitutes the fundamental problem to which we must address ourselves. If the mean value of the occupation number of the j th residue is obtained as a function of time, we can relate it to the helix content of the j th residue by

$$f_{\text{hd}}(j) = (1 + q_j)/2 \quad (\text{II-13})$$

Following the identical procedure employed in the derivation of eq II-12a and II-12b, we find that r_{jk} obeys

$$\alpha^{-1} \frac{dr_{j,k}(t)}{dt} = - \left\{ 2r_{j,k} - \frac{\gamma}{2}(r_{k,j-1} + r_{k,j+1} + r_{j,k-1} + r_{j,k+1}) - \delta(r_{j,k^0} + r_{k,j^0}) + \frac{\gamma\delta}{2}(\langle \mu_k \mu_j \mu_{j-1}^0 \rangle + \langle \mu_k \mu_j \mu_{j+1}^0 \rangle + \langle \mu_j \mu_k \mu_k^0 \mu_{k+1} \rangle + \langle \mu_j \mu_k \mu_k^0 \mu_{k-1} \rangle) - \beta(q_j + q_k) + \frac{\beta\gamma}{2}(\langle \mu_k \mu_{j-1} \mu_j \rangle + \langle \mu_k \mu_j \mu_{j+1} \rangle + \langle \mu_j \mu_{k-1} \mu_k \rangle + \langle \mu_j \mu_k \mu_{k+1} \rangle) + \beta\delta(\langle \mu_j \mu_k^0 \mu_k \rangle + \langle \mu_j \mu_j^0 \mu_k^0 \rangle) - \frac{\beta\gamma\delta}{2}(\langle \mu_k \mu_j^0 \mu_{j-1} \rangle + \langle \mu_k \mu_j^0 \mu_{j+1} \rangle + \langle \mu_j \mu_k^0 \mu_{k-1} \rangle + \langle \mu_j \mu_k^0 \mu_{k+1} \rangle) \right\} \quad (\text{II-14})$$

An analogous expression holds for the time dependence r_{j^0,k^0} and is obtained by interchanging superscripted and nonsuperscripted variables. Since the two chains are by hypothesis identical, we have $r_{j,k}(t) = r_{j^0,k^0}(t)$. Finally, we have

$$\alpha^{-1} \frac{dr_{j,k^0}}{dt} = - \left\{ 2r_{j,k^0} - \frac{\gamma}{2}(r_{j-1,k^0} + r_{j+1,k^0} + r_{j,k^0-1} + r_{j,k^0+1}) - 2\delta r_{j,k} + \frac{\gamma\delta}{2}(\langle \mu_k^0 \mu_j^0 \mu_{j-1} \rangle + \langle \mu_k^0 \mu_j^0 \mu_{j+1} \rangle + \langle \mu_j \mu_k \mu_k^0 \mu_{k-1}^0 \rangle + \langle \mu_j \mu_k \mu_k^0 \mu_{k+1}^0 \rangle) - \beta(q_j + q_k) + \frac{\beta\gamma}{2}(\langle \mu_k^0 \mu_j \mu_{j-1} \rangle + \langle \mu_k^0 \mu_j \mu_{j+1} \rangle + \langle \mu_j \mu_k^0 \mu_{k-1}^0 \rangle + \langle \mu_j \mu_k^0 \mu_{k+1}^0 \rangle) + \beta\delta(\langle \mu_j \mu_j^0 \mu_k^0 \rangle + \langle \mu_j \mu_k \mu_k^0 \rangle) - \frac{\beta\gamma\delta}{2}(\langle \mu_k^0 \mu_j^0 \mu_{j-1} \rangle + \langle \mu_k^0 \mu_j^0 \mu_{j+1} \rangle + \langle \mu_j \mu_{k-1}^0 \mu_k \rangle + \langle \mu_j \mu_k \mu_{k+1}^0 \rangle) \right\} \quad (\text{II-15})$$

Equations II-12b, II-14, and II-15 are applicable to homopolymeric, two-chain, coiled coils of arbitrary degree of polymerization; the construction of a closure relation for the coupled hierarchy which will enable us to obtain $q_j(t)$ is our next objective. However, before proceeding to the solution of the infinite-chain case, section III, we examine a limiting case of eq II-12a.

Reduction to the DNA-Isomorphic Model. While it is true that on the average for a homopolymeric, two-chain, coiled coil $\langle \mu_j(t) \rangle = \langle \mu_j^0(t) \rangle$, let us make the further assumption that the instantaneous values of $\mu_j(t) = \mu_j^0(t)$; i.e., we require at every instance in time that the j th residue in both chains be in the same conformational state. It immediately follows from eq II-12b on setting $\mu_j(t) = \mu_j^0(t)$ that

$$\frac{dq_j}{dt} = -\alpha(1-\delta) \left\{ q_j - \frac{\gamma}{2}(q_{j-1} + q_{j+1}) - \beta + \frac{\beta\gamma}{2}(r_{j,j-1} + r_{j,j+1}) \right\} \quad (\text{II-16})$$

which is precisely the master equation for the occupation number in a single-chain polypeptide having a fundamental rate constant $\alpha(1-\delta)$. Since $\delta \geq 0$ (see eq II-9d) this implies that the fundamental rate in a DNA-isomorphic chain is a factor $(1-\delta)$ slower than in the single-chain polypeptide ($\delta = 0$). This makes sense physically. In the DNA-isomorphic model, the j th residue in both chains must simultaneously undergo a conformational

transition. This process clearly must occur at best as fast as or, even more likely, slower than the analogous process for the j th residue in a single isolated homopolypeptide chain.

In the limit where $\beta = 0$ (i.e., at the midpoint of the transition for an infinite-chain homopolypeptide with $s = 1$, or a DNA-isomorphic model with $s(w^0)^{1/2} = 1$) there is an exact analytical solution valid for arbitrary degree of polymerization for both $q_j(t)$ and $q_j(\infty)$, the finite time and equilibrium value; we proceed to construct both below.

Equilibrium Solution: DNA-Isomorphic Model. For a single chain when $s = 1$ or equivalently for a DNA-isomorphic chain when $s(w^0)^{1/2} = 1$, the $t = \infty$ solution to eq II-16 satisfies the finite difference equation

$$q_j(\infty) = \frac{\gamma}{2}(q_{j-1}(\infty) + q_{j+1}(\infty)) \quad (\text{II-17})$$

wherein $\gamma < 1$ and is subject to the constraint that

$$q_0 = q_N = -1$$

Let us define

$$\cosh \theta = 1/\gamma \quad (\text{II-18})$$

Then it follows from the addition properties of hyperbolic functions that

$$q_j = -\cosh((N/2 - j)\theta) / \cosh(N\theta/2) \quad (\text{II-19})$$

Moreover, the mean occupation number defined by

$$\bar{q} = \frac{1}{N-1} \sum_{j=1}^{N-1} q_j \quad (\text{II-20a})$$

is

$$\bar{q} = (N-1)^{-1} \frac{(\sigma^{1/2} - 1/\sigma^{1/2}) \left[1 - \left(\frac{1 - \sigma^{1/2}}{1 + \sigma^{1/2}} \right)^{N-1} \right]}{1 + \sigma^{1/2} + (1 - \sigma^{1/2}) \left(\frac{1 - \sigma^{1/2}}{1 + \sigma^{1/2}} \right)^{N-1}} \quad (\text{II-20b})$$

Equation II-20b follows when eq II-20a is inserted into eq II-19 and the summation is performed. This is in agreement with the result obtained from the matrix formulation of the one-dimensional Ising model.⁴¹

Observe from eq II-19 that for j on the order of $N/2$, i.e., for the j th residue in the middle of a chain, and in the limit $N \rightarrow \infty$, $q_j \rightarrow 0$; that is, the average value of the occupation number is zero and the probability that the j th residue is helical is one-half. When $s = 1$ in single chains and $s(w^0)^{1/2} = 1$ in a DNA-isomorphic model in the limit of a very long chain, a residue is just as likely to be in the helix state as in the randomly coiled state; $\bar{q} = \bar{q}_j = 0$. It also follows from eq II-20b that $\bar{q} \rightarrow 0$ as $N\sigma^{1/2} \rightarrow \infty$.

Time-Dependent Solution: DNA-Isomorphic Model. In the case of a single-chain polypeptide when $s = 1$ or for a DNA-isomorphic dimer with $s(w^0)^{1/2} = 1$, we have

$$\alpha^{-1}(1-\delta)^{-1} \frac{dq_j}{dt} = - \left\{ q_j - \frac{\gamma}{2}(q_{j+1} + q_{j-1}) \right\} \quad (\text{II-21})$$

wherein δ is defined in eq II-9c. Equation II-21 is in the form of a finite difference equation, the solution of which is⁴²

$$q_j(t) = q_j(\infty) + \frac{2}{N} \sum_{m=1}^{N-1} \sum_{k=1}^{N-1} (q_k(0) - q_k(\infty)) \sin \frac{m\pi k}{N} \sin \frac{m\pi j}{N} e^{-\nu_m t} \quad (\text{II-22a})$$

in which $q_j(0)$ ($q_j(\infty)$) is the value of the occupation number of the j th residue at time zero (infinity). Moreover the m th relaxation rate is given by

$$\nu_m = \alpha(1 - \delta) \left\{ 1 - \gamma \cos \frac{m\pi}{N} \right\}; \quad 1 \leq m \leq N - 1 \quad (\text{II-22b})$$

Let us now calculate the value of the mean occupation number at time t .

$$\bar{q}(t) = \frac{1}{N-1} \sum_{j=1}^{N-1} q_j(t) \quad (\text{II-23a})$$

Now, the sum

$$\sum_{j=1}^{N-1} \sin \frac{m\pi j}{N} = \frac{(1 - (-1)^m) \cos(m\pi/2N)}{2 \sin(m\pi/2N)} \quad (\text{II-23b})$$

Thus we have

$$\bar{q}(t) = \bar{q}(\infty) + \frac{2}{(N)(N-1)} \sum_{m=1}^{N-1} \sum_{k=1}^{N-1} e^{-\nu_m t} (q_k(0) - q_k(\infty)) \frac{\sin \frac{m\pi k}{N} \cos \frac{m\pi}{2N}}{\sin \frac{m\pi}{2N}} \quad (\text{II-23c})$$

where the prime in the summation over m indicates a sum over odd m only. Thus, any measurement of the mean occupation number as a function of time only probes the relaxation times corresponding to odd modes and is completely transparent to the even modes.

As we shall demonstrate in a forthcoming paper, the general form of eq II-22a and II-23c is carried over to the approximate time-dependent solution in the more general case for $s \neq 1$ for single chains and as well as for the two-chain, coiled coil. A similar result for the autocorrelation function in single chains has been obtained by Tanaka, Wada, and Suzuki.³¹ For the DNA-isomorphic model and for single-chain homopolymers, eq II-22a is exact provided that $\beta = 0$ and is valid for all initial conditions, i.e., any arbitrary value of $q_j(0)$, and is not restricted to small perturbations from equilibrium.

The initial slope is readily obtained from eq II-22a or from eq II-11 evaluated at $t = 0$ and is given by

$$\left. \frac{dq_j}{dt} \right|_{t=0} = -\alpha(1 - \delta) \left\{ q_j(0) - \frac{\gamma}{2} (q_{j+1}(0) + q_{j-1}(0)) \right\} \quad (\text{II-24})$$

Thus, as mentioned previously, the initial slope is trivially obtained from the model and depends only on the properties of state at $t = 0$ and on the kinetic parameters δ and γ .

Equation II-22a may be expressed in terms of modified Bessel functions of the first kind $I_m(z)$ ⁴³ if we use

$$e^{z \cos \theta} = I_0(z) + 2 \sum_{s=1}^{\infty} I_s(z) \cos(s\theta) \quad (\text{II-25a})$$

Inserting eq II-25a into eq II-22a and carrying out the requisite summations gives

$$q_j(t) - q_j(\infty) = e^{-\alpha(1-\delta)t} \sum_{k=1}^{N-1} (q_k(0) - q_k(\infty)) \sum_{l=-\infty}^{+\infty} I_{j-k+2Nl}(\alpha(1-\delta)\gamma t) \quad (\text{II-25b})$$

a form similar to that obtained by Glauber for the average spin on a ring if $q_k(\infty) = 0$.⁴⁰ The factor $2Nl$ reflects the difference boundary conditions applicable here; while Glauber requires periodic boundary conditions, we require $q_0 = q_N = -1$.

Extension to the $N = \infty$ Limit. Letting $N \rightarrow \infty$ in eq II-22a, we can collapse the double sum in eq II-22a into a single sum if we recognize that

$$\sin \frac{m\pi k}{N} \sin \frac{m\pi j}{N} = \frac{1}{2} \left\{ \cos \frac{m\pi(k-j)}{N} - \cos \frac{m\pi(k+j)}{N} \right\} \quad (\text{II-26a})$$

and convert the sum over m into an integral. After a bit of arithmetic manipulation we arrive at

$$q_j(t) - q_j(\infty) = e^{-\alpha(1-\delta)t} \sum_{k=1}^{N-1} (q_k(0) - q_k(\infty)) \{ I_{k-j}(z) - I_{k+j}(z) \} \quad (\text{II-26b})$$

Wherein $z = \alpha(1 - \delta)\gamma t$. Moreover, if k lies near the middle of the chain we note that $q_k(\infty) = 0$ and assuming $q_k(0) = q(0)$, it follows that for residues far removed from the chain ends

$$q(t) = q(0) e^{-\alpha(1-\delta)t} \sum_{r=1-j}^{N-1-j} I_r(z) \quad (\text{II-27a})$$

In limit that $N \rightarrow \infty$, using eq II-25a we obtain the simple result that

$$q(t) = q(0) e^{-\alpha(1-\delta)(1-\gamma)t} \quad (\text{II-27b})$$

i.e., the solution to eq II-21 assuming $q_j(t) = q$ independent of j . Observe that q_j relaxes with a characteristic rate $\alpha(1 - \gamma)(1 - \delta)$.

Summarizing the results of this section, we have presented the kinetic Ising model version of the perfect-matching neglect-loop-entropy theory and have derived the master equation for the time dependence of the mean occupation number of the j th residue assuming that detailed balance holds at all times. We then considered a simplified kinetic model of the dimer, the time-dependent version of the DNA-isomorphic model, in which we required that the instantaneous occupation number of both chains be the same; that is, the j th residue in both chains must be in the identical conformational state. This model is equivalent to the kinetic Ising model of single-chain polypeptides with renormalized kinetic parameters. The fundamental rate constant of the DNA-isomorphic model is a factor $2/(1 + (w^0)^{1/2})$ slower than that in the corresponding single-chain polypeptide. Moreover, we derived an exact expression for $q_j(t)$ valid for any initial condition and arbitrary degree of polymerization provided that the final state of the DNA-isomorphic model or single chain corresponds to the transition midpoint in the infinite-chain limit; i.e., $s(w^0)^{1/2} = 1$ or $s = 1$, respectively. We have also demonstrated that the initial slope of this class of models reflects the properties of the initial state and kinetic parameters; eq II-9b-d. In the following section we shall turn to the more general solution for an arbitrary initial and final state of the less restrictive neglect-loop-entropy model.

III. Perfect-Matching Neglect-Loop-Entropy Kinetic Ising Model in the Infinite-Chain Limit

Before attempting to uncouple the hierarchy of differential equations for arbitrary initial and final state and for arbitrary degree of polymerization, it is most instructive to solve the simpler problem of an infinite two-chain, coiled coil to elucidate some of the general aspects of the dynamics. Moreover, any approximate solution we shall formulate for finite N must be consistent with the $N = \infty$ solution. Thus insight gained in studying the dynamics of a system without end effects should prove quite useful in the study of finite-chain systems.

$$A = \begin{bmatrix} 2 & -\gamma & 0 & \dots \\ -\gamma & 2 & -\gamma & \dots \\ 0 & -\gamma & 2 & -\gamma \dots \\ \vdots & \vdots & \vdots & \vdots \end{bmatrix} \quad (III-9d)$$

i.e., **A** is a tridiagonal matrix with 2 along the diagonal, $-\gamma$ on the first off-diagonal elements, and zero every place else. Writing

$$u = \begin{bmatrix} u_0 \\ v \end{bmatrix} \quad (III-10)$$

In Appendix C the eigenvalue equation

$$M u = \lambda u \quad (III-11a)$$

is solved for **u** and **u**⁺ (the left eigenvector) and the smallest eigenvalue λ provided that λ lies outside the spectral band of **A**. If this does not hold then λ is mixed in with the eigenvalues of **A** and we have not been able to construct an analytic solution for λ . However, if λ lies outside the spectral band of **A**, that is, either $\lambda < 2(1 - \gamma)$ or $\lambda > 2(1 + \gamma)$ (in our case the physically reasonable value of λ corresponds to the former rather than the latter condition), then from eq C-4c and C-7b, λ satisfies

$$(1 - \gamma - \lambda) + 2\beta^2\gamma(1 - \gamma)/(x - \gamma) = 0 \quad (III-11b)$$

wherein

$$x = \frac{2 - \lambda + ((2 - \lambda)^2 - 4\gamma^2)^{1/2}}{2} \quad (III-11c)$$

Expressions for the left and right eigenvectors of **M** corresponding to the eigenvalue λ are found in eq C-9b, C-13, and C-14. On the basis of these equations we conclude that the eigenvector corresponding to λ is a localized mode in the subspace of site and site-site correlation functions.

Several observations are appropriate at this time. First of all when $\beta = 0$ (i.e., when $s = 1$) we recover the exact expression for relaxation rate of the occupation number of an infinite chain, i.e., $\lambda = (1 - \gamma)$, and eq III-7c reduces to

$$q(t) - q(\infty) = (q(0) - q(\infty))e^{-\alpha(1-\gamma)t} \quad (III-12)$$

(Remember that $q(\infty) = 0$.)

Second, for any value of $|\beta| > 0$, λ must increase. Physically this represents the fact that nonzero β couples the relaxation of $\phi(t)$ into faster relaxing modes (the higher order correlation functions of the occupation number), the slowest of which relaxes as $2(1 - \gamma)$. Thus λ must have a minimum at $s = 1$; see Figure 1. If the relaxation spectrum is dominated by λ , then the relaxation time will have a maximum at $s = 1$, that is, symmetric in β (however, it is not symmetric in s ; see eq II-9d for the definition of β). When $s = 1$, since the free energy is an even function of the occupation number and the transition probability $\omega(\mu_j)$ is related to the equilibrium probability of the occupation numbers by detailed balance, odd (even) functions of the occupation number can only couple to other odd (even) functions; i.e., they reflect the equilibrium structure imposed by the free energy. The simplest form couples the mean occupation number to itself (see eq II-21). Thus coupling between even and odd functions of the occupation number are symmetry forbidden. Setting $\beta \neq 0$ breaks the symmetry and thus even and odd functions can couple. A nonzero β reflects the bias toward final state helix contents in the limit of infinite chains different from 50%. These conclusions are true in general and are not dependent on the specific approximations employed to solve either the DNA-isomorphic or neglect-loop-entropy model

and are a consequence of the form of the free energy of the system, eq II-2.

Third, if $q(t) - q(\infty)$ is significantly larger than $r_m(0) - r_m(\infty)$, then we would expect that

$$\frac{q(t) - q(\infty)}{q(0) - q(\infty)} = \frac{\sum_{l=1}^{\infty} S_{1l} S_{1l}^{-1} \Psi_l(0) e^{-\alpha \lambda_l t}}{(q(0) - q(\infty))} = C_{1s} e^{-\alpha \lambda t} \quad (III-13)$$

This reflects the fact that for values of σ where our approximation is valid, r_m is a fairly insensitive function of s . Take, for example, the extreme limit of complete helix \rightarrow complete coil; while $q(0)$ goes from 1 to -1 , r_m is identically unity in both cases. Thus, except for small perturbations from equilibrium where all the terms in eq III-7c are of the same order, we expect $\phi > \psi_j$. In other words, two-site correlation functions are slightly perturbed from their equilibrium values and relax very quickly whereas the mean occupation number is substantially perturbed and relaxes more slowly to equilibrium. Thus the time dependence of $q(t)$ will be characterized to a large extent by the smallest eigenvalue of **M**, namely, λ . In section IV, we shall numerically demonstrate that the aforementioned discussion is valid provided that the initial and final states are sufficiently far apart.

Two-Chain, Coiled Coils. In the case of two-chain, coiled coils, as seen in eq II-12b, II-14, and II-15, we have a more complicated set of equations to solve. The following approximations are all motivated by the fact that for systems likely to be encountered the two nearest-neighbor residues are likely to have the same instantaneous occupation number and are likely to flip simultaneously. Thus, we approximate in the $N \rightarrow \infty$ limit

$$\langle \mu_j \mu_j^0 \mu_{j\pm 1} \rangle \simeq q \quad (III-14)$$

in eq II-12b. We point out that the ratio $\langle \mu_j \mu_j^0 \mu_{j+1} \rangle / q$ calculated at equilibrium using eq B-12a if $s = 0.94$ and $\sigma = 10^{-4}$ varies from 0.9940 with $f_{hd} = 2.4 \times 10^{-2}$ and monotonically increases to 0.9969 with $f_{hd} = 0.992$ as w^0 is increased from 1.0 to 1.20. Thus throughout the entire range of helix content eq III-14 is a very good approximation to $\langle \mu_j \mu_j^0 \mu_{j-1} \rangle$.

In a similar fashion, in eq II-14, we approximate

$$\langle \mu_k \mu_j^0 \mu_{j\pm 1} \mu_j \rangle = \langle \mu_k \mu_j^0 \rangle \quad (III-15a)$$

and on setting $k = j + m$ we have

$$\langle \mu_k \mu_j^0 \mu_{j\pm 1} \mu_j \rangle = r_m^0(t) \quad (III-15b)$$

The superscript zero indicates a cross-correlation function between residues in two different chains. Furthermore, we employ as in the single-chain case eq III-2a and

$$\langle \mu_k \mu_j^0 \mu_{j\pm 1} \rangle \simeq q \quad (III-15c)$$

We have calculated the ratio $\langle \mu_{j-1} \mu_j^0 \mu_{j+1} \rangle / q$ for $s = 0.94$ and $\sigma = 10^{-4}$ as a function of w^0 . On increasing w^0 from 1.0 to 1.2, this ratio monotonically increases from 0.9886 to 0.9942. The $m \rightarrow \infty$ limit of the ratio $\langle \mu_{j+m} \mu_j^0 \mu_{j+1} \rangle / q$ is $\langle \mu_j^0 \mu_{j+1} \rangle$, which starts out at 0.9051, decreases to a minimum of about 0.84 at $s(w^0)^{1/2} = 1$, and increases to 0.9721 when $w^0 = 1.20$. Thus, the approximation of eq III-15c is a fairly reasonable one.

Moreover, in eq II-15 we replace

$$\langle \mu_k \mu_j \mu_j^0 \mu_{j\pm 1} \rangle \simeq \langle \mu_j^0 \mu_k^0 \rangle \quad (III-16a)$$

$$\simeq r_m(t) \quad (III-16b)$$

and

$$\langle \mu_k \mu_j^0 \mu_{j\pm 1} \rangle \simeq q \quad (III-17)$$

Let us define

$$\psi_m^0 = r_m^0(t) - r_m^0(\infty) \quad (\text{III-18})$$

Thus, we have on subtracting the $t = \infty$ limit from the approximate form of eq II-12b

$$\alpha^{-1} \frac{d\phi}{dt} = -\{(1-\gamma)(1-\delta)\phi + \beta\gamma\psi_1 + \beta\delta\psi_0^0 - \beta\gamma\delta\psi_1^0\} \quad (\text{III-19})$$

Setting $m = 1$ we have from eq II-14

$$\alpha^{-1} \frac{d\psi_1}{dt} = -\{2\psi_1 - \gamma\psi_2 + (-2\delta + \gamma\delta)\psi_1^0 + \gamma\delta\psi_0^0 - 2\beta(1-\gamma)(1-\delta)\phi\} \quad (\text{III-20a})$$

and for all $m > 1$

$$\alpha^{-1} \frac{d\psi_m}{dt} = -\{2\psi_m - \gamma[\psi_{m-1} + \psi_{m+1}] - 2\delta(1-\gamma)\psi_m^0 - 2\beta(1-\gamma)(1-\delta)\phi\} \quad (\text{III-20b})$$

It follows from eq II-15 and III-16a-d that

$$\alpha^{-1} \frac{d\psi_0^0}{dt} = -\{2\psi_0^0 - 2\gamma\psi_1^0 + 2\gamma\delta\psi_1 - 2\beta(1-\gamma)(1-\delta)\phi\} \quad (\text{III-21a})$$

and if $m > 1$

$$\alpha^{-1} \frac{d\psi_m^0}{dt} = -\{2\psi_m^0 - \gamma(\psi_{m-1}^0 + \psi_{m+1}^0) - 2\delta(1-\gamma)\psi_m - 2\beta(1-\gamma)(1-\delta)\phi\} \quad (\text{III-21b})$$

in which we recognize that $\psi_0(t) = 0$.

Now as in the case of the single chain, we can write the general solution to the set of coupled linear equations (III-19) to (III-21) by

$$\Phi(t) = e^{-\alpha \mathbf{D}t} \Phi(0) \quad (\text{III-22a})$$

where in the $2l \times 2l$ representation of \mathbf{D} we have

$$\Phi(t) = \begin{bmatrix} \phi \\ \psi_1 \\ \vdots \\ \psi_{l-1} \\ \psi_0^0 \\ \vdots \\ \psi_{l-1}^0 \end{bmatrix} \quad (\text{III-22b})$$

and in which the nonzero elements of \mathbf{D} are given in Appendix D; we then let $l \rightarrow \infty$ to obtain the complete set. In practice, we shall evaluate the finite l representation of \mathbf{D} and keep on doubling the dimension of the matrix until we obtain a result for $\phi(t)$ that is essentially independent of l .

It is more convenient just as in the single-chain case to use (see eq III-7c ff) the following form:

$$\Phi(t) = \mathbf{T}_d e^{-\alpha \Lambda_d t} \mathbf{T}_d^{-1} \Phi(0) \quad (\text{III-23})$$

in which the rows (columns) in \mathbf{T}_d^{-1} (\mathbf{T}_d) are the left (right) eigenvectors of \mathbf{D} and in which

$$[e^{-\alpha \Lambda_d t}]_{ij} = e^{-\alpha \lambda_{id} t} \delta_{ij} \quad (\text{III-24})$$

Λ_d is the diagonalized form of \mathbf{D} whose (1, 1) element contains the smallest (slowest relaxing mode) eigenvalue λ_{1d} .

Unfortunately, we have not been able to construct an analytic solution for λ_{1d} . As we shall see in the numerical

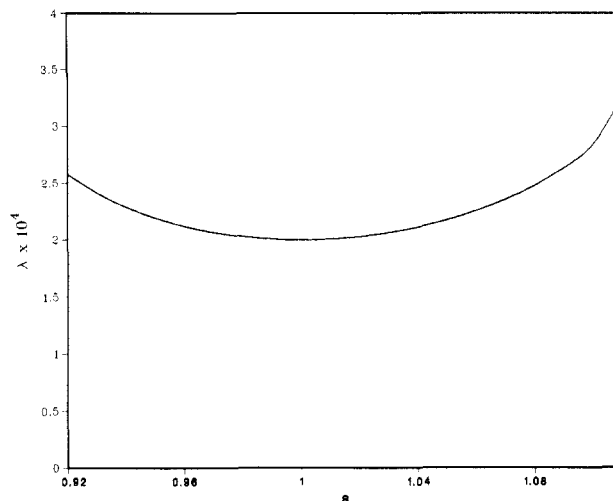


Figure 1. Plot of $\lambda \times 10^4$, the smallest eigenvalue of \mathbf{M} calculated from eq III-11b, vs. s for a single-chain homopolyptide of infinite length; $\sigma = 10^{-4}$.

results section, many but not all of the essential qualitative features of the single-chain case carry over to the neglect-loop-entropy-kinetic-Ising model of α -helical, two-chain, coiled coils. We would expect that for initial and final states that are sufficiently separated

$$\frac{q(t) - q(\infty)}{q(0) - q(\infty)} \cong \frac{\sum_{l=1}^{\infty} T_{d_{11}} T_{d_{1l}}^{-1} e^{-\alpha \lambda_{ld} t}}{\sum_{l=1}^{\infty} T_{d_{11}} T_{d_{1l}}^{-1}} / (q(0) - q(\infty)) = C_{1d} e^{-\alpha \lambda_{1d} t} \quad (\text{III-25})$$

Summarizing the results of this section, we have presented a numerically tractable solution of the kinetics of the helix-coil transition in α -helical, two-chain, coiled coils, in the limit of infinite chain length. On the basis of physically reasonable approximations we have closed the infinite set of coupled equations at the level of site-site (two point) correlation functions. At the level of site-site closure we have a set of equations that includes the full infinite set of two-site correlation functions. In the case of a single chain (or equivalently the DNA-isomorphic model) we have also derived analytic expressions for the eigenvalue and eigenvectors corresponding to the slowest relaxing mode, valid over the range of interest of the helix-coil transition. In the following section we shall obtain numerical results.

IV. Numerical Results

In this section we shall quantitatively substantiate the general qualitative picture presented in the previous section. We shall begin with a discussion of the simpler DNA-isomorphic model (single chains) with $\delta = 0$ and then turn to the more complicated two-chain, coiled-coil problem. In all cases calculations were done on infinite chains, i.e., chains sufficiently long that end effects may be neglected.

In Figure 1 we have plotted λ determined from eq III-11b vs. s where $0.92 \leq s \leq 1.11$ and $\sigma = 1 \times 10^{-4}$. Over this range of s the helix content increases from 1.38% to 99.1%, thereby clearly bracketing the range of interest. Observe that λ has a minimum precisely at $s = 1.0$ and assumes the exact value $(1-\gamma)$ equal to 1.9998×10^{-4} appropriate to the $\beta = 0$ case. (See eq II-27b.) The increase in λ reflects the coupling into faster relaxing two-site correlation functions possible when the symmetry of the free energy is broken. We finally observe that replacing λ by the value at $s = 1$ is a fairly good approximation in the range $0.95 \leq s \leq 1.05$ where the helix content goes from 3.4% to 96.3%.

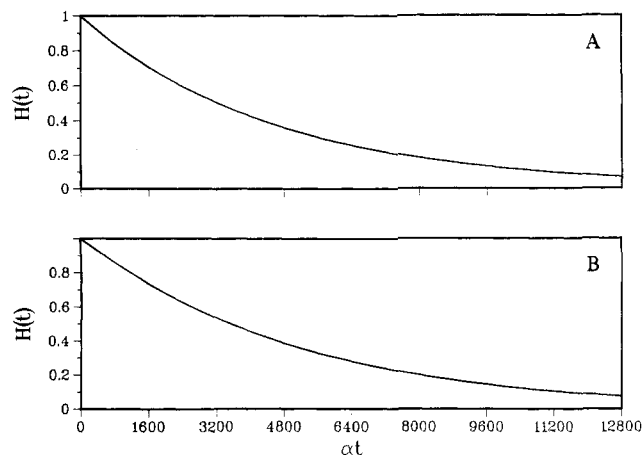


Figure 2. (A) Plot of $H(t)$, the normalized time-dependent helix content, vs. αt obtained from eq III-8 for a single-chain homopolymer of infinite length employing the 140×140 dimensional representation of \mathbf{M} . The initial state was $s_i = 0.97$, with helix content 8.2%, and the final state was $s_f = 1.04$, with helix content 94.5%. $\sigma = 10^{-4}$. (B) Plot of $H(t)$, the normalized time-dependent helix content, vs. αt obtained from eq III-8 for a single-chain homopolymer of infinite length employing the 140×140 dimensional representation of \mathbf{M} . The initial state was $s_i = 1.04$, with helix content 94.5%, and the final state was $s_f = 0.97$, with helix content 8.2%. $\sigma = 10^{-4}$.

On comparing the time dependence of the helix content between various different initial and final states, it is more appropriate to examine the normalized time-dependent helix content

$$H(t) = \frac{f_{\text{hd}}(t) - f_{\text{hd}}(\infty)}{f_{\text{hd}}(0) - f_{\text{hd}}(\infty)} \quad (\text{IV-1a})$$

or equivalently

$$H(t) = \frac{q(t) - q(\infty)}{q(0) - q(\infty)} \quad (\text{IV-1b})$$

In all the calculations presented below we have set $\sigma = 10^{-4}$. Identical qualitative behavior is seen for somewhat larger and smaller values of σ .

In Figure 2A we have plotted $H(t)$ vs. αt obtained from eq III-8 for a single chain corresponding to an initial state $s_i = 0.97$ with helix content 8.2% and a final state $s_f = 1.04$ with a helix content of 94.5%. The presented curve corresponds to the diagonalization of the 140×140 matrix representation of \mathbf{M} . We have also calculated $H(t)$ vs. αt obtained from diagonalization of 40×40 , 80×80 , 120×120 , and 140×140 matrices. Taking the value of $H(t)$ at $\alpha t = 12800$ as a measure of the convergence, we find the 80×80 result for $H(t)$ is within 4.5% of the 140×140 result and the 120×120 result is within 1.2% of the 140×140 result; thus a 140×140 result has essentially converged. The exact smallest eigenvalue is 2.1110×10^{-4} ; the calculated eigenvalue is 2.082×10^{-4} . The initial slope is 2.214×10^{-4} . We have also multiplied $H(t)$ by $e^{\alpha t}$; for all $\alpha t > 5800$ this ratio is a constant and is equal to C_{1s} . In fact over the entire range of αt , $H(t)$ is within 3% of the curve obtained by approximating $H(t)$ by $C_{1s}e^{-\alpha t}$. Hence, given the closeness of the initial slope and smallest eigenvalue, the renaturation of the helix from an initial state of small helix content is well characterized by the smallest eigenvector and eigenvalue.

Let us now consider the kinetics of unfolding of the helix. In Figure 2B we have plotted $H(t)$ vs. αt calculated from eq III-8 for a single chain where $s_i = 1.04$, $s_f = 0.97$, and $\sigma = 10^{-4}$. $H(t)$ is calculated with a 140×140 matrix representation of \mathbf{M} . On increasing the dimension of \mathbf{M} from 80×80 to 140×140 , $H(t)$ at $\alpha t = 12800$ decreases

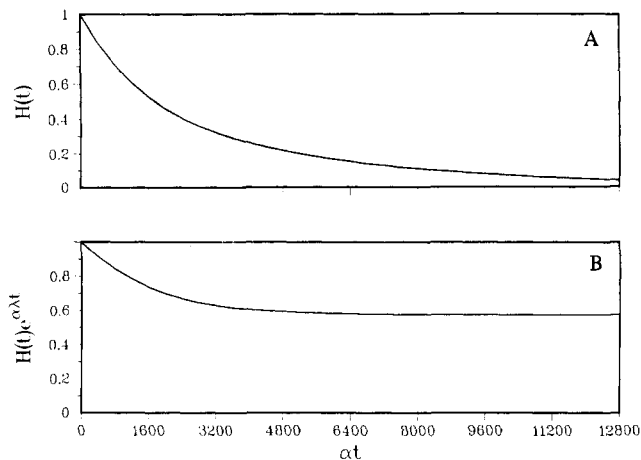


Figure 3. (A) Plot of $H(t)$, the normalized time-dependent helix content, vs. αt obtained from eq III-8 for a single-chain homopolymer of infinite length employing the 140×140 dimensional representation of \mathbf{M} . The initial state was $s_i = 1.001$, with helix content 52.5%, and the final state was $s_f = 1.04$, with helix content 94.5%. $\sigma = 10^{-4}$. (B) Plot of $H(t)e^{\alpha t}$ vs. αt for the same conditions as in (A). The $t = \infty$ asymptotic limit (see eq III-13) is 0.5759.

by about 0.5%, indicating very good convergence. The smallest eigenvalue is 2.049×10^{-4} , which is to be compared with the exact value of 2.066×10^{-4} corresponding to the infinite-dimensional representation of \mathbf{M} . Clearly, the two are in very close agreement. Furthermore, the initial slope is 1.833×10^{-4} . Multiplication of $H(t)$ by $e^{\alpha t}$ gives in the limit of large times 1.030, the asymptotic value of C_{1s} . In fact, over the entire range $H(t)e^{\alpha t}$ is within 3% of the slowest relaxing mode approximation. Again for the unfolding kinetics of a single chain, we conclude the smallest eigenvalue approximation to $H(t)$ is very good.

The reader will observe that the smallest eigenvalue λ for the $s_f = 1.04$ state is 2.110×10^{-4} whereas for the $s_f = 0.97$ state λ equals 2.066×10^{-4} . Thus, the kinetics of folding for the particular case chosen is slightly faster than the kinetics of unfolding. Basically as shown in Figure 1, λ is an even function of β (see eq III-11b), having a minimum value at $\beta = 0$ (no bias at equilibrium for the helix or coil states) and increasing for nonzero β . When $s_f = 1.04$, $\beta = 0.0196$ whereas when $s_f = 0.97$, $\beta = 0.0152$. Of course, we can arbitrarily arrange it such that λ associated with the nearly helical state is less than λ associated with the low-helix state. Basically, in the infinite-chain limit for the values of s chosen the dynamics is dominated by the cooperativity of the transition, with a rate essentially given by $\alpha(1 - \gamma)$. This implies that on the average the j th residue and its neighbors are in the same state and uniformly approach the $t = \infty$ limit; thus we have a case where helical and coil states are treated equivalently and the rate is characteristic of the final state.

We should however point out that if s_f is sufficiently small, the above conclusion will no longer be true if helix initiation becomes the rate-determining step. However, since chains of interest seem to retain a residual helix content of about 10% at high temperature,⁵⁻⁹ this case need not concern us here. We now turn to the case where the initial and final states are not so widely separated.

In Figure 3A we have plotted $H(t)$ vs. αt employing eq III-8 for a single chain with initial state $s_i = 1.001$ and a helix content 52.5% and final state having $s_f = 1.04$ and helix content 94.5%. On diagonalizing the 140×140 matrix representation of \mathbf{M} , we find an initial slope of 4.538×10^{-4} , whereas the smallest eigenvalue is 2.082×10^{-4} . In Figure 3B we plot $H(t)e^{\alpha t}$ vs. αt . Clearly, the curve does not approach the C_{1s} limit (=0.5759) until a substantial portion of the relaxation has already occurred. Thus the

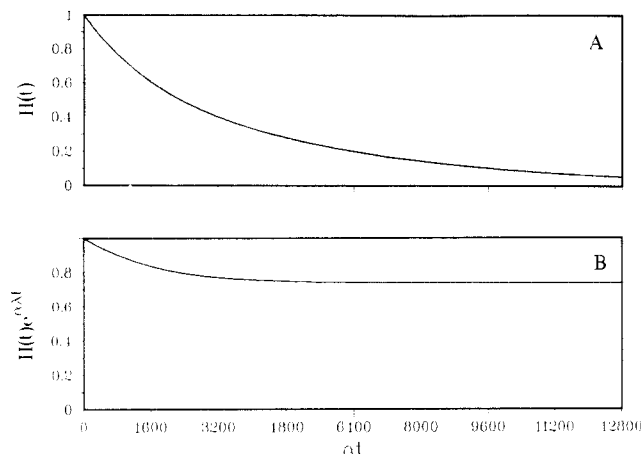


Figure 4. (A) Plot of $H(t)$, the normalized time-dependent helix content, vs. αt obtained from eq III-8 for a single-chain homopolymer of infinite length employing the 140×140 dimension representation of \mathbf{M} . The initial state was $s_i = 1.001$, with helix content 52.5%, and the final state was $s_f = 0.97$, with helix content 8.2%. $\sigma = 10^{-4}$. (B) Plot of $H(t)e^{\alpha\lambda t}$ vs. αt for the same conditions as (A). The $t = \infty$ asymptotic limit (see eq III-13) is 0.7367.

greater initial slope reflects the stronger coupling into the faster relaxing modes, a characteristic of a "quasi-equilibrium" experiment. Basically, as $q(0)$ and $q(\infty)$ lie closer together the amplitude factors corresponding to the faster relaxing modes and $q(0) - q(\infty)$ are closer in magnitude. Thus, the initial slope becomes larger.

It should be pointed out that for the maximum dimensional matrix we can conveniently diagonalize (140×140) on the IBM 370/158 computer, the larger eigenvalues have not converged to the $l \rightarrow \infty$ limit. While the initial slope is independent of l , the dimension of the matrix, C_{1s} has not quite converged to the $l \rightarrow \infty$ value. Thus, in fact the $l \rightarrow \infty$ limit of $H(t)$ vs. αt will decay even faster than the approximate $l = 140$ results of Figure 3. The results presented here are qualitatively useful in that they point out the difference between a base line to base line experiment, where the initial and final states correspond to high and low helix or vice versa, which just probes the slowest relaxing mode, and, for $s \neq 1$, the quasi-equilibrium experiment, which probes a much broader relaxation spectrum. The final state $s_f = 1$ probes the slowest relaxing mode and gives a relaxation rate of the same order of magnitude as a base line to base line experiment.

In Figure 4A we have plotted $H(t)$ vs. αt calculated employing eq III-8 for a single chain in initial state $s_i = 1.001$ with helix content 52.5% and $s_f = 0.97$ with helix content 8.2%. On diagonalizing the 140×140 matrix representation of \mathbf{M} , the initial slope is found to be 3.546×10^{-4} whereas the smallest eigenvalue is 2.049×10^{-4} . In this case as compared to the situation examined in Figure 3, the convergence to the $l \rightarrow \infty$ limit is better; nevertheless a 140×140 matrix is not in the $l \rightarrow \infty$ limit. In Figure 4B we have plotted $H(t)e^{\alpha\lambda t}$ vs. αt . The asymptotic limit of C_{1s} is equal to 0.7367 and is not reached until a substantial portion of relaxation of $H(t)$ from unity has occurred. Again as in the case of relaxation from a moderate-helical state to a high-helical state, the relaxation behavior of $H(t)$ vs. αt of the moderate helix to low helix transition is more complicated than a base line to base line experiment and probes to a greater extent a broader range of relaxation rates. We shall return to these points in greater detail following consideration of the dimer dynamics.

We now turn to the kinetics of the helix-coil transition in α -helical, two-chain, coiled coils. It is apparent from

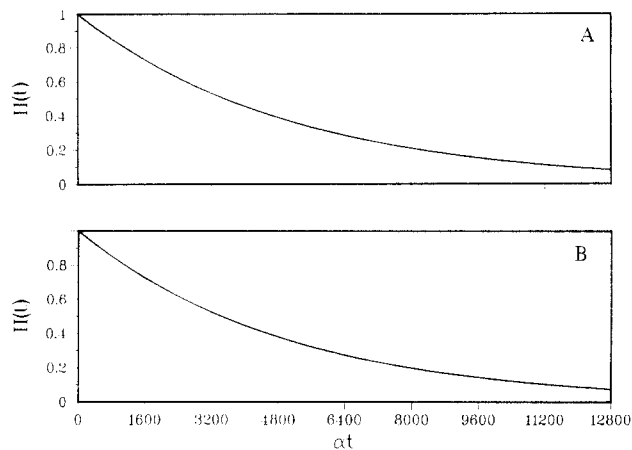


Figure 5. (A) Plot of $H(t)$ vs. αt calculated via eq III-23 for an infinite two-chain, coiled coil with initial state $w_i^0 = 1$ and helix content 8.2% and final state $w_f^0 = 1.08$ and helix content 90.5%. A 140×140 dimension representation of \mathbf{D} was used. $\sigma = 10^{-4}$ and $s = 0.97$. (B) Plot of $H(t)$ vs. αt calculated via eq III-23 for an infinite two-chain, coiled coil with initial state $w_i^0 = 1.08$ and helix content 90.5% and final state $w_f^0 = 1.0$ and helix content 8.2%. A 140×140 dimension representation of \mathbf{D} was used. $\sigma = 10^{-4}$ and $s = 0.97$.

Appendix D that setting $\beta = 0$ gives $\lambda = (1 - \gamma)(1 - \delta)$ at the midpoint of the transition, a result identical to that obtained in eq II-27b for the DNA-isomorphous model. Thus, for a given value of s characteristic of the isolated single chain, $\lambda_{1d} = (1 - \gamma)[2s/(1 + s)]$. Since by hypothesis $s < 1$ for an isolated single chain, we have for the final state corresponding precisely to the midpoint of the transition that the two-chain, coiled coil has a λ_{1d} that is a factor $2s/(1 + s)$ smaller than that of a single chain whose final state is 50% helix, assuming the same value of σ in the single chain as the dimer. Taking, for example, the case where $s = 0.97$, the ratio of λ_{1d} to λ (single chain) is 0.985; and if $\sigma = 10^{-4}$, $\lambda_{\text{dimer}} = 1.96935 \times 10^{-4}$ for the transition to the state corresponding to 50% helix content. This slowest relaxing mode reflects the cooperative nature of the transition. It is a long-wavelength mode in which the average value of the occupation number is the same for the j th residue and its neighbors. The dynamics involves the cooperative transition of a large number of residues on the order of $1/\sigma^{1/2}$. Thus we conclude that in this model infinite single chains and infinite two-chain, coiled coils have base line to base line kinetics that occur on the same time scale.

For all cases considered below, we have set s equal to 0.97 and σ equal to 10^{-4} . In Figure 5A we present $H(t)$ vs. αt calculated employing eq III-23 for the two-chain, coiled coil with an initial state where $w_i^0 = 1$ with helix content 8.2% and a final state $w_f^0 = 1.08$ with helix content 90.5%. We have diagonalized \mathbf{D} defined in Appendix D, taking $l = 20$, $l = 40$, and $l = 70$ (i.e., matrices of dimension 40×40 , 80×80 , and 140×140). On going from $l = 20$ to $l = 70$, when $\alpha t = 12800$, the two values of $H(t)$ differ by less than 0.3%. Clearly, the smallest eigenvalue has converged. Moreover, virtually the entire $H(t)$ vs. αt curve is given by $C_{1d}e^{-\alpha\lambda_{1d}t}$ wherein $\lambda_{1d} = 1.963 \times 10^{-4}$; moreover, the initial slope is quite close to λ_{1d} , with a value of 1.983×10^{-4} . Finally, we point out that the value of λ_{1d} is essentially identical with the smallest eigenvalue obtained when $s(w^0)^{1/2} = 1$, with the slight decrease reflecting the role of positive δ , i.e., the increased cooperativity of the transition.

In Figure 5B we have plotted $H(t)$ vs. αt employing eq III-23 for a two-chain, coiled coil in which the initial state has $w_i^0 = 1.08$ with helix content 90.5% and the final state

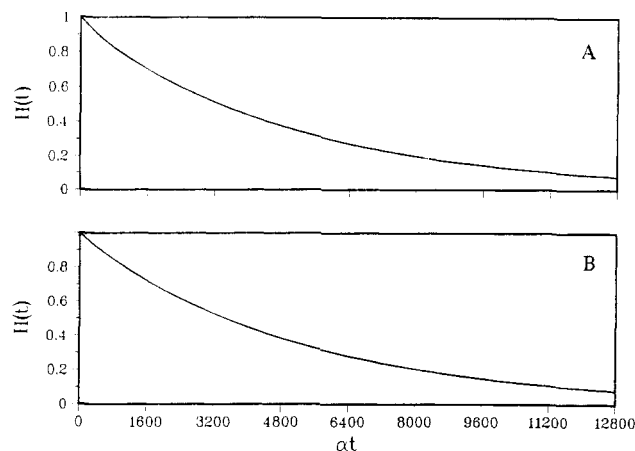


Figure 6. (A) Plot of $H(t)$ vs. αt calculated via eq III-23 for an infinite two-chain, coiled coil with initial state $w_i^0 = 1.075$ and helix content 85.2% and final state $w_f^0 = 1.08$ and helix content 90.5%. A 140×140 dimension representation of **D** was used. $\sigma = 10^{-4}$ and $s = 0.97$. (B) Plot of $H(t)$ vs. αt calculated via eq III-23 for an infinite two-chain, coiled coil with initial state $w_i^0 = 1.075$ and helix content 85.2% and final state $w_f^0 = 1.07$ and helix content 75.1%. A 140×140 dimension representation of **D** was used. $\sigma = 10^{-4}$ and $s = 0.97$.

has $w_f^0 = 1.0$ and helix content 8.2%. We have calculated $H(t)$ vs. αt with $l = 20$, $l = 40$, and $l = 70$. When $\alpha t = 12800$, $H(t)$ calculated with $l = 40$ and $l = 70$ differed by 2.3%; so, clearly, $l = 70$ is quite close to the $l = \infty$ limit. As in the previous case, virtually the entire $H(t)$ vs. αt curve is characterized to within 0.43% by $C_{1d}e^{-\alpha\lambda_{1d}t}$ wherein $\lambda_{1d} = 2.029 \times 10^{-4}$ and $C_{1d} = 1.0044$. The initial slope is 1.919×10^{-4} . Furthermore, λ_{1d} obtained employing eq III-23 when $l = 40$ is 2.0174×10^{-4} and is identical with λ , the smallest eigenvalue for the infinite single chain obtained from eq III-8, when $l = 40$, thereby demonstrating that the method for two-chain, coiled coils reduces to the single-chain limit for the smallest eigenvalue when $w_f^0 = 1$.

It is readily apparent from Figure 5 that this model predicts that the time scale for helix-to-coil transitions or vice versa is quite similar for the base line to base line kinetics in both single chains and two-chain, coiled coils. While the transition to near-complete helix in two-chain, coiled coils is slightly slower, the rate differs by a few percent at most. Thus, on the basis of the present section we conclude that (a) for transitions between widely separated initial and final states, the $H(t)$ curve is essentially given by $C_{1d}e^{-\alpha\lambda_{1d}t}$. (b) For ranges of the helix content between 8% and 90%, λ_{1d} is well approximated by $(1 - \gamma)(1 - \delta)$; thus, experiments with measure $H(t)$ therefore probe the slowest relaxing mode.

Consider now the case where the initial and final states are not quite so widely separated. In particular, in Figure 6A we plot $H(t)$ vs. αt calculated employing eq III-23 with $l = 70$ for an initial state $w_i^0 = 1.075$ with helix content 85.2% and final state $w_f^0 = 1.08$ and helix content 90.5%. The initial slope in this case is found to be 2.590×10^{-4} , whereas λ_{1d} is 1.963×10^{-4} . Moreover, the calculated values are quite close to the $l \rightarrow \infty$ limit; on increasing l from 40 to 70, the values of $H(t)$ at $\alpha t = 12800$ agree to within 3%. Moreover, the value $H(t)e^{\alpha\lambda_{1d}t}$ fairly quickly converges to C_{1d} and $H(t)$ is given by $C_{1d}e^{-\alpha\lambda_{1d}t}$ for times beyond $\alpha t = 1700$. Otherwise stated, while the initial slope has increased as compared to the $w_i^0 = 1.0$ and $w_f^0 = 1.08$ case, the $H(t)$ vs. αt relaxation curve is still dominated by the slowly relaxing mode and lies within 5% of the value $C_{1d}e^{-\alpha\lambda_{1d}t}$ at all times. This is in striking contrast to the single-chain dynamics shown in Figures 3 and 4, where

changes in helix content of about 40% produce an appreciable increase in the initial slope. Here for changes in helix content of 5%, the $H(t)$ vs. αt curve still probes the slowest relaxing mode.

To examine whether the approximation of $H(t)$ by $C_{1d}e^{-\alpha\lambda_{1d}t}$ also holds for denaturation, we have plotted $H(t)$ vs. αt in Figure 6B with an initial state $w_i^0 = 1.075$ and a helix content 85.2% and a final state $w_f^0 = 1.07$ and a helix content 75.1%. Here, too, we have a similar case as in Figure 6A; the initial slope is 2.136×10^{-4} whereas the smallest eigenvalue is 1.966×10^{-4} . The entire relaxation curve is well approximated by $C_{1d}e^{-\alpha\lambda_{1d}t}$. Moreover, convergence to the $l = \infty$ limit is good, with the value of $H(t)$ at $\alpha t = 12800$ within 0.8% of its value on increasing l from 40 to 70.

We have also done a series of calculations for initial and final states very close to each other. We set $w_i^0 = 1.081$ and $w_f^0 = 1.08$; this corresponds to an initial-state helix content of 91.3% and a final-state helix content of 90.5%. In this case, the initial slope is 2.748×10^{-4} whereas $\lambda_{1d} = 1.963 \times 10^{-4}$. The value of $H(t)$ at $\alpha t = 12800$ where $l = 40$ lies within 5% of the value when $l = 70$. Hence, the convergence to the $l = \infty$ limit is fairly good, but not excellent. $H(t)$ vs. αt is within 6% of the limiting behavior given $C_{1d}e^{-\alpha\lambda_{1d}t}$ over the entire curve and appears very well approximated by this form for αt greater than 3400, i.e., for values of $H(t)$ less than 0.50. This calculation demonstrates that for dimers as in single chains for perturbations sufficiently close to the initial state, the faster relaxing modes are probed at short time and make a substantial contribution to the relaxation spectrum; however, this occurs for perturbations from the initial state that are substantially smaller in the dimer than in the single chain.

The reason that the dimer relaxation spectrum probes the slowest relaxing mode over a broader range of initial states with the same final state has its origin in the relative magnitudes of the amplitude factors $q(0) - q(\infty)$ as compared to $r_m(0) - r_m(\infty)$ and for dimers, $r_m^0(0) - r_m^0(\infty)$. When $q(0) - q(\infty) \gg r_m(0) - r_m(\infty)$, i.e., when the site-site correlation functions are slightly perturbed from their equilibrium values while the occupation numbers (helix content) of the initial and final states are substantially different, the slowest relaxing mode dominates the relaxation behavior of $H(t)$. The faster relaxing modes will make important contributions to $H(t)$ when $q(0) - q(\infty)$ becomes on the order of $r_m(0) - r_m(\infty)$. In dimers, this occurs for much smaller values of $q(0) - q(\infty)$ than for single chains. This can be rationalized quite simply. As pointed out in previous work⁴⁴ the helix-coil transition in infinite two-chain, coiled coils is more cooperative than the corresponding transition at identical σ for single chains. This is equivalent to saying that dimers have a smaller effective helix initiation parameter—which in turn means at a given difference in helix content that $r_m(0)$ and $r_m(\infty)$ will be closer in dimers than in single chains (as $\sigma \rightarrow 0$, $r_m \rightarrow 1$). Thus the fact that the difference in initial and final states in the dimer must be smaller than in the single chain to probe the faster relaxing modes (assuming of course $\beta \neq 0$) is a reflection of difference in equilibrium properties of the two systems.

Several additional observations are appropriate at this time. One way of probing $H(t)$ is to do a temperature-jump experiment in which one typically goes through the helix-coil transition in uniform 5 °C increments. Since at low and high temperature the helix content vs. T curves are flat, one is really probing a small deviation from equilibrium, with attendant large initial slope and smaller

mean relaxation time. Thus, at very low and high temperature the temperature-jump experiment probes a broader spectrum of relaxation times.

Consider now the same 5 °C temperature jump in the vicinity of the midpoint of the helix-coil transition, where the slope of the $f_{hd}(T)$ vs. T curve is large and the initial and final states are more widely separated. Here, one may in fact be probing the slowest relaxing mode. Not surprisingly then, since the temperature-jump experiment produces a different perturbation from the initial state depending on the temperature, different relaxation processes are probed. The theory indicates that it is especially true for two-chain, coiled coils, but also for single chains, that the rate associated with a base line to base line transition may be estimated by examining the rate obtained in a quasi-equilibrium experiment whose final state is the transition midpoint. Furthermore, the plot of mean relaxation time vs. temperature should have a maximum at the transition midpoint, in qualitative agreement with the experiments of Tsong, Himmelfarb, and Harrington.¹² Hence we conclude that qualitatively at least the kinetic Ising model description of the helix-coil transition in two-chain, coiled coils is in accord with experiment.

V. Discussion of Results

In this paper, we have begun the theoretical examination of the helix-coil transition of α -helical, two-chain, coiled coils. To render the mathematics tractable, we have focused on the simplest kinetic Ising model of the dynamics which we believe contains the essence of many aspects of the physics. That is, we have treated the helix-coil (and vice versa) kinetics of parallel, in-register dimers in which the effects of loop entropy are entirely disregarded, the kinetic Ising neglect-loop-entropy model. We have focused explicitly on homopolymeric chains. Employing these approximations we have formulated the master equation for the mean occupation number of the j th residue, q_j . Analytic expressions for q_j are derived for the limiting cases of an isolated single chain as well as for the DNA-isomorphous model for chains of arbitrary length where the equilibrium final state corresponds to $s = 1$ and $s(w^0)^{1/2} = 1$, respectively. We then turned to consideration of the infinite-chain limit of single chains and two-chain, coiled coils having arbitrary initial and final states. Physically reasonable approximations are introduced to close the infinite set of coupled differential equations, equations that couple correlation functions of the occupation numbers between all sets of residues. This allowed us to reduce the problem to consideration of coupled linear first-order differential equations involving the mean occupation number q and all orders of the site-site correlation functions $\langle \mu_j \mu_{j+m} \rangle$, $m = 1, 2, \dots, \infty$. Thus, we have reduced the problem to that of diagonalizing matrices. In the case of isolated single chains we have derived an analytic expression for the smallest eigenvalue and associated eigenvectors valid over a fairly wide range of helix content. For two-chain, coiled coils the calculation of $q(t)$ depends on the numerical determination of the eigenvectors and eigenvalues of the coupling matrix. Thus formally, at least, the time dependence of the helix content at this level of approximation is solved.

These important qualitative results emerge from the actual numerical analysis for infinite chains. First, the time scale for the slowest relaxing mode over a fairly wide range of helix content in single chains and in dimers is essentially the same; the rate for the slowest relaxing mode in dimers is slightly smaller than in single chains. Second, the relaxation rate that corresponds to the slowest relaxing mode in single chains has a maximum at the midpoint of the

helix-coil transition and for both single chains and dimers is quite flat over the experimentally significant range of helix contents. Thus probing the kinetics of the transition to 50% helix content allows one to estimate the rate of transition from an initial state with very low helix content to a final state with fairly high helix content or vice versa. Third, for infinite chains, at least for helix contents in the range of a few percent to 90%, the dominant process corresponding to the slowest relaxing mode is a cooperative long-wavelength motion in which domains of length on the order of $1/\sigma^{1/2}$ flip on the average in the direction of the appropriate equilibrium state. Fourth, the slowest relaxing mode dominates the kinetics of the helix-coil transition in the dimer for a larger range of initial states than in a single chain having the same helix initiation parameter. This is entirely due to the more cooperative nature of the helix-coil transition in dimers as compared to single chains. Finally, temperature-jump experiments employing a uniform change in temperature probe the quasi-equilibrium regime at low and high temperature and probe large perturbations from equilibrium in the vicinity of the transition midpoint.

Clearly, at this point, much work remains to be done. In a future publication, we shall extend the present treatment to finite chains. The next step involves inclusion of the effects of loop entropy, but not mismatch, a treatment which will have many elements in common with the kinetic zipper model³³⁻³⁵ employed previously in polypeptides and polynucleotides. The subsequent step, the inclusion of mismatch, is more formidable, as is the treatment of the dynamics if diffusion between single chains occurs on the same time scale as the helix-coil kinetics. Thus, while the present work has provided qualitative insight into some of the important features of the helix-coil transition kinetics in two-chain, coiled coils, it is by no means definitive.

Acknowledgment. This research was supported in part by a grant from the Biophysics Program of the National Science Foundation (No. PCM-8212404). Thanks are due to Professors Holtzer and Yaris for many stimulating and useful discussions.

Appendix A. Equivalence of the Single-Chain Ising Model and Zimm-Bragg Model of the Helix-Coil Transition

In the Ising model developed in section II, to relate the parameters J and H to the Zimm-Bragg σ and s we had to append two phantom random coil units at the end of the chain. Thus

$$\sum_{j=1}^N (\mu_{j-1} - \mu_j) = \mu_0 - \mu_N = 0 \quad (\text{A-1})$$

Adding eq A-1 to eq II-2 leaves the free energy unchanged and gives

$$\mathcal{H}_1 = -J \sum_{j=1}^N (\mu_j \mu_{j-1} + \mu_{j-1} - \mu_j) - H \sum_{j=0}^N \mu_j \quad (\text{A-2})$$

Equation A-2 gives the statistical weight matrix

$$U_{mi} = \begin{matrix} & \begin{matrix} c & h \end{matrix} \\ \begin{matrix} c \\ h \end{matrix} & \begin{vmatrix} 1 & \sigma s \\ 1 & s \end{vmatrix} \end{matrix} \quad (\text{A-3})$$

if $1 \leq i \leq N-1$ and the corresponding partition function

$$Z_m = \text{row}(1, 0) \prod_{i=1}^{N-1} U_{mi} \text{col}(1, 1) \quad (\text{A-4})$$

thus showing the equivalency of this particular variant of

the equilibrium Ising model and Zimm-Bragg theory provided that the chain is homopolymeric. In general, as Poland and Scheraga have pointed out,⁴¹ the general one-dimensional Ising model and Zimm-Bragg theory differ only in their treatment of single helical states; as shown here for our specific case the two models are equivalent and we can use the formalism developed previously to construct equilibrium averages.

Appendix B. Equilibrium Correlation Functions in the $N \rightarrow \infty$ Limit

Let us begin with the ensemble average of the two-site correlation function

$$\langle \mu_j \mu_{j+1} \rangle = \frac{\mathbf{J}^* \prod_{i=1}^{j-1} \mathbf{U}_{di} \mathbf{A}_\mu \mathbf{A}_\mu \prod_{i=j+2}^{N-1} \mathbf{U}_{di} \mathbf{J}}{\mathbf{J}^* \prod_{i=1}^{N-1} \mathbf{U}_{di} \mathbf{J}} \quad (\text{B-1})$$

\mathbf{J}^* and \mathbf{J} are row (1, 0, 0, 0) and col (1, 1, 1, 1) vectors, respectively, wherein \mathbf{U}_{di} is the statistical weight matrix of the i th pair of residues in the dimer

$$\mathbf{U}_{di} = \mathbf{U}_{mi} \otimes \mathbf{U}_{mi} \mathbf{E}_w \quad (\text{B-2})$$

\mathbf{U}_{mi} is defined in eq A-3 and is the statistical weight matrix of the i th residue in an isolated single chain, \otimes denotes the direct product, and \mathbf{E}_w is a diagonal matrix with unity everywhere on the diagonal except $E_w(4,4) = w$. Furthermore

$$\mathbf{A}_\mu = \begin{bmatrix} -1 & \sigma s \\ -1 & s \end{bmatrix} \otimes \mathbf{U}_{mi} \mathbf{E}_w \quad (\text{B-3})$$

is the statistical weight matrix that calculates the mean occupation number of the i th residue in chain 1.

Let us employ the similarity transformation that diagonalizes \mathbf{U}_d (see ref 44).

$$\mathbf{T}^{-1} \mathbf{U}_d \mathbf{T} = \lambda \quad (\text{B-4})$$

λ is a diagonal matrix whose largest eigenvalue $\lambda(1,1)$ is λ_+ . For a homopolymeric, two-chain, coiled coil in the limit that $N \rightarrow \infty$, end effects need not be considered and we may replace eq B-1 by

$$r_1 = \langle \mu_j \mu_{j+1} \rangle = \text{Trace} [\lambda^{j-1} \mathbf{T}^{-1} \mathbf{A}_\mu^2 \mathbf{T} \lambda^{N-j-2}] / \text{Trace} \lambda^{N-1} \quad (\text{B-5})$$

Now in the limit of large j we can rewrite eq 5 as

$$\langle \mu_j \mu_{j+1} \rangle = \lambda_+^{-2} [\mathbf{T}^{-1} \mathbf{A}_\mu^2 \mathbf{T}]_{11} \quad (\text{B-6a})$$

In the more general case, we have

$$r_m = \langle \mu_j \mu_{j+m} \rangle = \lambda_+^{-(m+1)} [\mathbf{T}^{-1} \mathbf{A}_\mu \mathbf{T} \lambda^{m-1} \mathbf{T}^{-1} \mathbf{A}_\mu \mathbf{T}]_{11} \quad (\text{B-6b})$$

We shall also have recourse to calculate the mean helix content of an infinite chain. It can be obtained either analytically⁴⁴ or numerically from

$$f_{\text{hd}} = \lambda_+^{-1} [\mathbf{T}^{-1} \mathbf{U}_d' \mathbf{T}]_{11} \quad (\text{B-7a})$$

$$\mathbf{U}_d' = \begin{bmatrix} 0 & \sigma s \\ 0 & s \end{bmatrix} \otimes \mathbf{U}_{mi} \mathbf{E}_w \quad (\text{B-7b})$$

An illustration of the two methods of calculating f_{hd} is appropriate. Setting $s = 0.94$, $\sigma = 10^{-3}$, and $w^0 = 1.10$, employing eq B-7a gives $f_{\text{hd}} = 0.302586124$ whereas the analytic formula for f_{hd} gives 0.302585886. Thus the two methods give six significant figure agreement, a conclusion that seems to hold for all calculations done to date.

q may be obtained either by using eq B-7b in conjunction with eq II-13 or by directly evaluating

$$q = \lambda_+^{-1} [\mathbf{T}^{-1} \mathbf{A}_\mu \mathbf{T}]_{11} \quad (\text{B-8})$$

In a similar fashion, the three-site correlation functions are given by

$$\langle \mu_{j-1} \mu_j \mu_{j+m} \rangle = \lambda_+^{-(m+2)} [\mathbf{T}^{-1} \mathbf{A}_\mu^2 \mathbf{T} \lambda^{m-1} \mathbf{T}^{-1} \mathbf{A}_\mu \mathbf{T}]_{11} \quad (\text{B-9})$$

We also have the need for correlation functions of occupation numbers in residues on different chains, the simplest of which is

$$\langle \mu_j \mu_j^0 \rangle = \frac{1}{\lambda_+} [\mathbf{T}^{-1} \mathbf{A}_{\mu\mu^0} \mathbf{T}]_{11} \quad (\text{B-10a})$$

in which

$$\mathbf{A}_{\mu\mu^0} = \begin{bmatrix} -1 & \sigma s \\ -1 & s \end{bmatrix} \otimes \begin{bmatrix} -1 & \sigma s \\ -1 & s \end{bmatrix} \mathbf{E}_w \quad (\text{B-10b})$$

For the two-site occupation number correlation function located on different chains and at different residues

$$\langle \mu_j \mu_{j+m}^0 \rangle = \lambda_+^{-(m+1)} [\mathbf{T}^{-1} \mathbf{A}_\mu \mathbf{T} \lambda^{m-1} \mathbf{T}^{-1} \mathbf{A}_{\mu^0} \mathbf{T}]_{11} \quad (\text{B-11a})$$

wherein

$$\mathbf{A}_{\mu^0} = \mathbf{U}_{mi} \otimes \begin{bmatrix} -1 & \sigma s \\ -1 & s \end{bmatrix} \mathbf{E}_w \quad (\text{B-11b})$$

Finally, we may require

$$\langle \mu_j \mu_j^0 \mu_{j+1} \rangle = \lambda_+^{-2} [\mathbf{T}^{-1} \mathbf{A}_{\mu\mu^0} \mathbf{A}_\mu \mathbf{T}]_{11} \quad (\text{B-12a})$$

and

$$\langle \mu_j \mu_{j+1} \mu_{j+m}^0 \rangle = \lambda_+^{-(m+1)} [\mathbf{T}^{-1} \mathbf{A}_\mu^2 \mathbf{T} \lambda^{m-2} \mathbf{T}^{-1} \mathbf{A}_{\mu^0} \mathbf{T}]_{11} \quad (\text{B-12b})$$

For computational convenience, it should be pointed out that if we define a general matrix

$$\mathbf{A}_{a_q, a_q^0} = \mathbf{U}_d \begin{bmatrix} a_q & 0 \\ 0 & 1 \end{bmatrix} \otimes \begin{bmatrix} a_q^0 & 0 \\ 0 & 1 \end{bmatrix} \quad (\text{B-13})$$

we recover \mathbf{A}_μ defined in eq B-3 if $a_q^0 = 1$ and $a_q = -1$, $\mathbf{A}_{\mu\mu^0}$ defined in eq B-10b if both a_q and a_q^0 are set equal to -1 , and \mathbf{A}_{μ^0} defined in eq B-11b if $a_q = +1$ and $a_q^0 = -1$. Finally, we recover \mathbf{U}_d' defined in eq B-7b if we set a_q equal to zero and a_q^0 equal to 1.

Appendix C. Smallest Eigenvalue and Associated Eigenvectors in DNA-Isomorphic Model

Equation III-11a for the smallest eigenvalue of \mathbf{M} may be rewritten as

$$(1 - \gamma)u_0 + \mathbf{B}\mathbf{v} = \lambda u_0 \quad (\text{C-1a})$$

$$\mathbf{C}u_0 + \mathbf{A}\mathbf{v} = \lambda \mathbf{v} \quad (\text{C-1b})$$

On eliminating \mathbf{v} using eq C-1b, we have

$$(1 - \gamma)u_0 + \mathbf{B}[\mathbf{A} - \lambda \mathbf{E}]^{-1} \mathbf{C}u_0 = \lambda u_0 \quad (\text{C-2a})$$

or

$$(1 - \gamma - \lambda) + 2\beta^2\gamma(1 - \gamma) \sum_{j=1}^{\infty} [\mathbf{A} - \lambda \mathbf{E}]_{1j}^{-1} = 0 \quad (\text{C-2b})$$

Thus the problem for the determination of λ hinges on our ability to invert $\mathbf{A} - \lambda \mathbf{E}$. Let us set up a series of recursion relations for the determinant D_l of the $l \times l$ matrix

$$\begin{bmatrix} 2 - \lambda & -\gamma & 0 & \dots \\ -\gamma & 2 - \lambda & -\gamma & \dots \\ 0 & \vdots & \vdots & \dots \\ & & -\gamma & 2 - \lambda \end{bmatrix} \quad (\text{C-3})$$

i.e., the finite l -dimensional representation of $\mathbf{A} - \lambda \mathbf{E}$.

Letting $D_0 = 1$, we find that

$$D_{l+1} = (2 - \lambda)D_l - \gamma^2 D_{l-1} \quad (\text{C-4a})$$

Writing

$$x_l = D_l/D_{l-1} \quad (\text{C-4b})$$

we have

$$x_{l+1} = 2 - \lambda - \gamma^2/x_l \quad (\text{C-4c})$$

In the limit that $l \rightarrow \infty$ it is possible to show that this is a continued fraction expansion which converges to the largest root of

$$x = 2 - \lambda - \gamma^2/x \quad (\text{C-4d})$$

provided that λ , the smallest eigenvalue of \mathbf{M} , lies outside the spectral band of \mathbf{A} ; $2(1 - \gamma) > \lambda$ or $2(1 + \gamma) < \lambda$. Namely

$$x = \frac{2 - \lambda + [(2 - \lambda)^2 - 4\gamma^2]^{1/2}}{2} \quad (\text{C-5})$$

Now, using the well-known relationship of the classical adjoint of a matrix and its inverse,⁴⁵ we have

$$[\mathbf{A} - \lambda\mathbf{E}]_{ij}^{-1} = \frac{\text{cof} [\mathbf{A} - \lambda\mathbf{E}]_{ji}}{\det [\mathbf{A} - \lambda\mathbf{E}]} \quad (\text{C-6a})$$

For an $l \times l$ matrix, it is straightforward to show that

$$[\mathbf{A} - \lambda\mathbf{E}]_{lj}^{-1} = \gamma^{j-1} D_{l-j}/D_l \quad (\text{C-6b})$$

which converges to

$$[\mathbf{A} - \lambda\mathbf{E}]_{lj}^{-1} = \gamma^{j-1} x^{-j} \quad (\text{C-6c})$$

Hence the equation for λ becomes

$$(1 - \gamma - \lambda) + 2\beta^2\gamma(1 - \gamma) \sum_{j=1}^{\infty} \gamma^{-1}(\gamma/x)^j = 0 \quad (\text{C-7a})$$

On explicitly summing the geometric series, we have

$$(1 - \gamma - \lambda) + 2\beta^2\gamma(1 - \gamma)/(x - \gamma) = 0 \quad (\text{C-7b})$$

which must be solved by employing eq C-5 for x as a function of λ .

We now proceed to determine the right and left eigenvectors of \mathbf{M} corresponding to the smallest eigenvalue λ . We begin with the construction of \mathbf{u}^t . Clearly \mathbf{u}^t satisfies the set of equations

$$u_0^t(1 - \gamma) + \mathbf{v}^t\mathbf{C} = \lambda u_0^t \quad (\text{C-8a})$$

$$u_0^t\mathbf{B} + \mathbf{v}^t\mathbf{A} = \lambda \mathbf{v}^t \quad (\text{C-8b})$$

Equations C-8a and C-8b can be used to show that λ , the smallest eigenvalue, is the same for both \mathbf{u} and \mathbf{u}^t , as is expected. Furthermore, eq C-8b gives

$$-u_0^t\mathbf{B}[\mathbf{A} - \lambda\mathbf{E}]^{-1} = \mathbf{v}^t \quad (\text{C-8c})$$

Let us set u_0 and u_0^t equal to unity. (We shall construct the normalized set of left and right eigenvectors below.) Then it immediately follows from eq C-8c that

$$v_j^t = -\beta\gamma[\mathbf{A} - \lambda\mathbf{E}]_{lj}^{-1} \quad (\text{C-9a})$$

and from eq C-6c we have

$$v_j^t = -\beta(\gamma/x)^j; \quad j \geq 1 \quad (\text{C-9b})$$

We now must determine \mathbf{v} . Setting u_0 equal to 1, we have from eq C-1b

$$-[\mathbf{A} - \lambda\mathbf{E}]^{-1}\mathbf{C} = \mathbf{v} \quad (\text{C-10a})$$

or written explicitly in terms of components

$$2\beta(1 - \gamma) \sum_{j=1}^{\infty} [\mathbf{A} - \lambda\mathbf{E}]_{ij} = v_i; \quad i \geq 1 \quad (\text{C-10b})$$

Now, in general, one can show that for the $l \times l$ representation of $[\mathbf{A} - \lambda\mathbf{E}]$

$$[\mathbf{A} - \lambda\mathbf{E}]_{ij}^{-1} = \gamma^{j-i} \frac{D_{l-j}D_{i-1}}{D_l} \quad \text{if } j \geq i \quad (\text{C-11a})$$

$$= \gamma^{i-j} \frac{D_{l-i}D_{j-1}}{D_l} \quad \text{if } i \geq j \quad (\text{C-11b})$$

so that in limit $l \rightarrow \infty$

$$[\mathbf{A} - \lambda\mathbf{E}]_{ij}^{-1} = \gamma^{j-i} x^{-j} D_{i-1} \quad \text{if } j \geq i \quad (\text{C-12a})$$

$$= \gamma^{i-j} x^{-i} D_{j-1} \quad \text{if } i > j \quad (\text{C-12b})$$

Inserting eq C-12a and C-12b into eq C-10b we have

$$v_i = \frac{2\beta(1 - \gamma)}{x^i} \left[\sum_{j=1}^{i-1} \gamma^{i-j} D_{j-1} + x \frac{D_{i-1}}{x - \gamma} \right] \quad (\text{C-13})$$

since $\gamma/x < 1$.

Equations C-9b and C-13 show that eigenvectors \mathbf{u} and \mathbf{u}^t are localized modes; that is, they decay exponentially with increasing j .

The various D_{i-1} and D_{j-1} may be obtained from eq C-4a. Finally, the normalized left and right eigenvectors are given by \mathbf{u}^t/N_l and \mathbf{u}/N_l , respectively, where the normalization factor

$$N_l^2 = 1 + \sum_{j=1}^{\infty} v_j v_j^t \quad (\text{C-14})$$

Appendix D. Nonzero Matrix Elements of \mathbf{D}

In the $2l \times 2l$ finite matrix representation, the nonzero matrix elements of \mathbf{D} are

$$D_{11} = (1 - \gamma)(1 - \delta) \quad (\text{D-1})$$

$$D_{12} = \beta\gamma \quad (\text{D-2})$$

$$D_{1,l+1} = \beta\delta \quad (\text{D-3})$$

$$D_{1,l+2} = -\beta\gamma\delta \quad (\text{D-4})$$

$$D_{i,1} = -2\beta(1 - \gamma)(1 - \delta); \quad i = 2, \dots, 2l \quad (\text{D-5})$$

$$D_{ii} = 2; \quad 2 \leq i \leq l \quad (\text{D-6})$$

$$D_{i,i-1} = -\gamma; \quad 2 \leq i \leq l \quad (\text{D-7})$$

$$D_{i,i+1} = -\gamma; \quad 2 \leq i \leq l - 1 \quad (\text{D-8})$$

$$D_{2,l+1} = \gamma\delta \quad (\text{D-9})$$

$$D_{2,l+2} = -2\delta(1 - \gamma/2) \quad (\text{D-10})$$

$$D_{i,l+i} = -2\delta(1 - \gamma); \quad i > 2 \quad (\text{D-11})$$

$$D_{l+1,2} = 2\gamma\delta \quad (\text{D-12})$$

$$D_{l+i,i} = -2\delta(1 - \gamma); \quad i \geq 2 \quad (\text{D-13})$$

$$D_{l+i,l+i} = 2 \quad (\text{D-14})$$

$$D_{l+1,l+2} = -2\gamma \quad (\text{D-15})$$

$$D_{l+i,l+i-1} = -\gamma; \quad i \geq 2 \quad (\text{D-16})$$

$$D_{l+i,l+i+1} = -\gamma; \quad 2 \leq i \leq l \quad (\text{D-17})$$

References and Notes

- (1) Skolnick, J.; Holtzer, A. *Macromolecules* **1982**, *15*, 303.
- (2) Skolnick, J. *Macromolecules* **1983**, *16*, 1069.
- (3) Skolnick, J. *Macromolecules* **1983**, *16*, 1763.

- (4) Skolnick, J. *Macromolecules* 1984, 17, 645.
 (5) Holtzer, M. E.; Holtzer, A.; Skolnick, J. *Macromolecules* 1983, 16, 173.
 (6) Holtzer, M. E.; Holtzer, A.; Skolnick, J. *Macromolecules* 1983, 16, 462.
 (7) Lehrer, S. *J. Mol. Biol.* 1978, 118, 209.
 (8) Woods, E. *Aust. J. Biol. Sci.* 1976, 29, 405.
 (9) Crimmins, D.; Isom, L.; Holtzer, A. *Comp. Biochem. Physiol. B* 1981, 69B, 35.
 (10) Potekhin, S.; Privalov, P. *J. Mol. Biol.* 1982, 159, 519.
 (11) Hodges, R.; Saund, A.; St. Pierre, S.; Reid, R. *J. Biol. Chem.* 1981, 256, 1214.
 (12) Tsong, T. Y.; Himmelfarb, S.; Harrington, W. F. *J. Mol. Biol.* 1983, 164, 431.
 (13) Schwarz, G. *Biopolymers* 1968, 6, 873.
 (14) Zimm, B.; Bragg, J. K. *J. Chem. Phys.* 1959, 31, 526.
 (15) (a) Vol'kenstein, M. V.; Gotlib, Y.; Ptitsyn, O. B. *Fiz. Tverdogo Tela* 1961, 3, 420. (b) Gotlib, Y. Y. *Fiz. Tverdogo Tela* 1961, 3, 2170.
 (16) Go, N. *J. Phys. Soc. Jpn.* 1967, 22, 416.
 (17) Craig, M. E.; Crothers, D. M. *Biopolymers* 1968, 6, 385.
 (18) Rawlings, P. K.; Schneider, F. W. *Ber. Bunsenges. Phys. Chem.* 1973, 77, 237.
 (19) Chay, T. R.; Stevens, C. L. *Macromolecules* 1975, 8, 531.
 (20) Silberberg, A.; Simha, R. *Biopolymers* 1968, 6, 479.
 (21) Rabinowitz, P.; Silberberg, A.; Simha, R.; Loftus, E. *Adv. Chem. Phys.* 1969, 15, 281.
 (22) Simha, R.; Silberberg, A. *Macromolecules* 1972, 5, 332.
 (23) Schwarz, G. *J. Mol. Biol.* 1965, 11, 64.
 (24) Poland, D.; Scheraga, H. A. *J. Chem. Phys.* 1966, 45, 2071.
 (25) Craig, M. E.; Crothers, D. M. *Biopolymers* 1968, 6, 385.
 (26) Lumry, R.; Legare, R.; Miller, W. G. *Biopolymers* 1964, 2, 486.
 (27) Barksdale, A.; Stuehr, J. *J. Am. Chem. Soc.* 1972, 94, 3334.
 (28) Zana, R.; Lang, J. *Biopolymers* 1973, 12, 79.
 (29) Schwarz, G.; Seelig, J. *Biopolymers* 1968, 6, 1263.
 (30) Wada, A.; Tanaka, T.; Kihara, H. *Biopolymers* 1972, 11, 587.
 (31) Tanaka, T.; Wada, A.; Suzuki, M. *J. Chem. Phys.* 1973, 59, 3799.
 (32) Ishiwari, K.; Nakajima, A. *Macromolecules* 1978, 11, 785 and references cited therein.
 (33) Chay, T. R.; Stevens, C. L. *Biopolymers* 1973, 12, 2563.
 (34) Miller, W. G. *Macromolecules* 1973, 6, 100.
 (35) (a) Jernigan, R. L.; Ferretti, J. A.; Weiss, G. H. *Macromolecules* 1973, 6, 684. (b) Jernigan, R. L.; Ferretti, J. A. *J. Chem. Phys.* 1975, 62, 2519.
 (36) McQuarrie, D. A.; McTague, J. P.; Reiss, H. *Biopolymers* 1965, 3, 657.
 (37) McLachlan, A.; Stuart, M. *J. Mol. Biol.* 1975, 98, 293.
 (38) Stone, D.; Smillie, L. *J. Biol. Chem.* 1978, 253, 1137.
 (39) Mak, A.; Lewis, W.; Smillie, L. *FEBS Lett.* 1979, 105, 232.
 (40) Glauber, R. J. *J. Math. Phys.* 1963, 4, 294.
 (41) Poland, D.; Scheraga, H. "Theory of Helix-Coil Transitions in Biopolymers"; Academic Press: New York, 1970.
 (42) Morse, P. M.; Feshbach, H. "Methods of Theoretical Physics"; McGraw-Hill: New York, 1953; p 133.
 (43) Abramowitz, M.; Stegun, I. A. "Handbook of Mathematical Functions"; Dover: New York, 1972; Chapter 9.
 (44) Skolnick, J. *Macromolecules* 1984, 17, 2153.
 (45) Byron, F.; Fuller, R. "Mathematics of Classical and Quantum Physics"; Addison-Wesley: Reading, MA, 1969; Vol. I.

Polylactones. 1. Copolymerization of Glycolide and ϵ -Caprolactone

Hans R. Kricheldorf,* Thomas Mang, and J. Michael Jonté

Institut für Angewandte Chemie der Universität, Martin-Luther-King-Platz 6, D-2000 Hamburg 13, FRG. Received December 5, 1983

ABSTRACT: Copolymerization of glycolide and ϵ -caprolactone was conducted in bulk at 100 °C and in nitrobenzene or dioxane at 70, 100, or 150 °C. The resulting copolyesters were characterized with respect to their molar composition by means of ^1H NMR spectra and with respect to their sequences by means of ^{13}C NMR spectra. The results allow a classification of both copolyesters and initiators. Cationic initiators such as ferric chloride, boron trifluoride, and fluorosulfonic acid favor the incorporation of ϵ -caprolactone, catalyze intermolecular transesterifications, and cause rapid degradation of the polyesters above 100 °C. Complexing catalysts such as zinc chloride, aluminum isopropylate, and dibutyltin dimethylate favor the incorporation of glycolide and chemical heterogeneity of first order. Furthermore, intramolecular transesterification was detected in the case of aluminum isopropylate and dibutyltin dimethylate. Anionic catalysts such as tetramethylammonium benzoate and benzyltriphenylphosphonium chloride only initiate the homopolymerization of glycolide. The polymerization mechanisms are discussed. The differential scanning calorimetry shows a close relationship between crystallinity and nature of sequences.

Introduction

Poly(glycolide) and copolymers of glycolide and LL-lactide have attracted much interest because of their usefulness in medicine, in particular as surgical sutures.¹⁻³ In addition to satisfactory mechanical properties these copolyesters have a low immunogenicity and an extremely low toxicity. Since interest in biodegradable polymers of low toxicity seems likely to increase in the future, copolyesters other than glycolide and lactide need to be investigated. Hydroxycaproic acid is another building block of relatively low toxicity and a suitable monomer is technically available in the form of ϵ -caprolactone. Poly(ϵ -caprolactone) and copolyesters of ϵ -caprolactone and D,L-lactide have been investigated, especially in regard to biodegradability and for use in drug delivery systems.⁴⁻⁷ Copolyesters built up of ϵ -caprolactone and glycolyl units are interesting because they allow a broad variation of their chemical and physical properties. Poly(glycolide) is a rigid, highly crystalline material with a melting point around 219

°C. It is insoluble in most organic solvents, including trifluoroacetic acid, and has a high crystal density (1.7 g/cm³). Poly(ϵ -caprolactone) is a more flexible material which has a low melting point (56 °C), a low crystal density (1.2 g/cm³), and good solubility in most organic solvents. To the best of our knowledge, copolyesters of glycolide and ϵ -caprolactone were never studied in detail. Thus, it was the purpose of the present paper to investigate various copolymerizations of glycolide and ϵ -caprolactone, to characterize the sequences by means of NMR spectroscopy, and to relate the sequence to the reaction mechanisms, on the one hand, and to properties, such as solubility and crystallinity, on the other hand.

Experimental Section

Monomers. ϵ -Caprolactone (EGA-Chemie, D-7924 Steinheim) was distilled under nitrogen over oligomeric 4,4'-diisocyanatodiphenylmethane. Glycolide was prepared by thermal condensation of sodium chloroacetate in the presence of copper turnings.⁸ It was washed with diethyl ether and recrystallized from dry